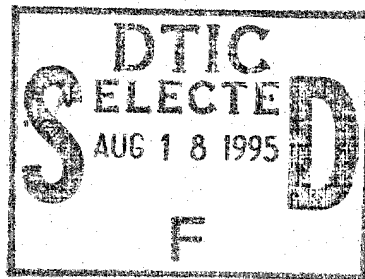


**Technical Report
1019**

Bragg Resonance in Measured L-Band Radar Clutter Doppler Spectra from Inland Water



J.B. Billingsley
J.F. Larrabee

1 August 1995

Lincoln Laboratory
MASSACHUSETTS INSTITUTE OF TECHNOLOGY
LEXINGTON, MASSACHUSETTS



Prepared for the Department of the Air Force and the Advanced Research
Projects Agency under Air Force Contract F19628-95-C-0002.

Approved for public release; distribution is unlimited.

DTIC QUALITY INSPECTED 5

19950816 126

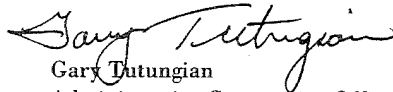
This report is based on studies performed at Lincoln Laboratory, a center for research operated by Massachusetts Institute of Technology. The work was sponsored by the Department of the Air Force and the Advanced Research Projects Agency under Air Force Contract F19628-95-C-0002.

This report may be reproduced to satisfy needs of U.S. Government agencies.

The ESC Public Affairs Office has reviewed this report, and it is releasable to the National Technical Information Service, where it will be available to the general public, including foreign nationals.

This technical report has been reviewed and is approved for publication.

FOR THE COMMANDER


Gary Tutungian
Administrative Contracting Officer
Contracted Support Management

MASSACHUSETTS INSTITUTE OF TECHNOLOGY
LINCOLN LABORATORY

**BRAGG RESONANCE IN MEASURED L-BAND RADAR CLUTTER
DOPPLER SPECTRA FROM INLAND WATER**

J.B. BILLINGSLEY

Group 105

J.F. LARRABEE

Loral Training and Technical Services

TECHNICAL REPORT 1019

1 AUGUST 1995

Approved for public release; distribution is unlimited.

LEXINGTON

MASSACHUSETTS

ABSTRACT

A highly developed Bragg resonance phenomenon was observed in measurements of vertically polarized L-band radar backscatter recorded from the surface of a small inland fresh-water reservoir in central Massachusetts. These measurements were obtained with Lincoln Laboratory's LCE (L-band Clutter Experiment) radar sited on Wachusett Mt. from which the reservoir surface was visible at 4-km range and at 4° depression angle, on a day of light winds with the radar looking obliquely downwind. The highly developed Bragg resonance in the backscatter from the reservoir surface caused strong Bragg spikes to exist in the clutter Doppler spectrum from the reservoir at low (viz., +3.4 and -3.8 Hz) but nonzero-Doppler frequencies. The sharp narrow first-order Bragg spikes rose 20 to 25 dB above adjacent spectral levels in the clutter spectra from the reservoir surface. The maximum amplitude of the dominant Bragg spike at -3.8 Hz was 40 to 45 dB stronger than tree clutter at -3.8 Hz in nearby spatial cells and only 10 dB weaker than the peak zero-Doppler tree clutter in the same nearby cells. This strong Bragg resonance at vertical polarization was persistent in time (15 min) and space (all seven range gates for which the reservoir surface was visible to the radar) throughout the course of measurements on the light-winds measurement day. Spectral results are presented for both cross-polarized and both copolarized combinations of linear polarization. Bragg spikes were observed to exist across this polarization matrix of measurements, although at horizontal polarization the overall backscatter from the reservoir surface, including the Bragg resonant component, was much weaker than at vertical polarization. On a second measurement day of stronger winds and changed wind direction (such that the radar was looking upwind), significant Bragg resonance still existed in the backscatter from the reservoir surface but was weaker than on the light-winds day. Strong Bragg spikes at low but nonzero-Doppler frequencies from small inland bodies of water might potentially cause false alarms for moving target indicator or other Doppler signal processing techniques designed for target detection in ground clutter.

Accession For	
NTIS CRA&I	<input checked="" type="checkbox"/>
DTIC TAB	<input type="checkbox"/>
Unannounced	<input type="checkbox"/>
Justification _____	
By _____	
Distribution /	
Availability Codes	
Dist	Avail and/or Special
A-1	

ACKNOWLEDGMENTS

The authors particularly acknowledge the dedicated efforts of Richard L. Ferranti, the LCE radar Project Engineer. Lewis A. Thurman and Curtis W. Davis III provided management direction. Ken Gregson, Reese Straw, and JoAnne Bradley assisted in data calibration and reduction. The manuscript was skillfully prepared by Pat DeCuir and Chris DeSesa and kindly and efficiently reviewed by C.E. Muehe, who provided a number of constructive suggestions.

TABLE OF CONTENTS

Abstract	iii
Acknowledgments	v
List of Illustrations	ix
1. INTRODUCTION	1
2. LCE RADAR INSTRUMENTATION	5
3. LCE MEASURED BRAGG RESONANCE RESULTS	9
3.1 Light Wind Conditions	9
3.2 Additional Range Gates	14
3.3 Persistence with Time and Polarization	16
3.4 Stronger Wind Conditions	19
4. DISCUSSION	27
4.1 Bragg Scattering in Sea Clutter	27
4.2 Context for Land Clutter	30
5. SUMMARY	37
REFERENCES	39

LIST OF ILLUSTRATIONS

Figure No.		Page
1	The LCE radar on Wachusett Mt.	1
2	View from the west shore across Mare Meadow Reservoir east to Wachusett Mt. in the distance.	2
3	Narrowest and widest LCE-measured spectra.	8
4	LCE-measured clutter power spectrum from the windblown fresh-water surface of Mare Meadow Reservoir showing strong Bragg resonances.	11
5	Figure 1(a) repeated with estimated ground clutter leakage through antenna sidelobes.	12
6	LCE-measured clutter amplitude temporal records.	13
7	LCE-measured clutter power spectra showing variations with range as range gate position traverses Mare Meadow Reservoir.	14
8	LCE-measured clutter power spectra from the surface of Mare Meadow Reservoir showing polarization variations.	17
9	LCE-measured clutter power spectra from the surface of Mare Meadow Reservoir for two similar experiments showing variation with time of measurement.	18
10	LCE-measured clutter power spectrum from the windblown fresh-water surface of Mare Meadow Reservoir showing Bragg resonances.	21
11	LCE-measured clutter power spectra from the surface of Mare Meadow Reservoir showing variations with wind condition on two different day.	22
12	LCE-measured clutter amplitude temporal records.	23
13	LCE-measured clutter power spectra showing variations with range as range gate position traverses Mare Meadow Reservoir.	24
14	LCE-measured clutter power spectra from the surface of Mare Meadow Reservoir showing polarization variations.	25
15	LCE-measured clutter power spectra from the surface of Mare Meadow Reservoir for two similar experiments showing variation with time of measurement.	26
16	Published measurements of HF sea clutter spectra showing strong Bragg resonances.	28
17	Phase One sea clutter measurements.	29
18	Three inland water clutter spectra.	31
19	Three ground clutter spectra from trees.	32
20	Inland water clutter versus tree clutter spectra.	33

1. INTRODUCTION

A highly developed Bragg resonance phenomenon has been observed in the vertically polarized L-band backscatter measured by Lincoln Laboratory's LCE (L-band Clutter Experiment) radar from the surface of an inland fresh-water reservoir. The radar was sited on top of Wachusett Mt. in central Massachusetts, approximately 1000 ft above the surrounding hilly forested terrain (see Figure 1). The backscatter was measured from Mare Meadow Reservoir, situated 3.97 km west (viz., $Az = 294^\circ$) of the radar at a grazing angle of 3.98° . Mare Meadow Reservoir is approximately 2 km long (north-south) by 0.6 km across (east-west) at its broadest point. Figure 2 is a photograph of Mare Meadow Reservoir taken from the west shore looking east across the reservoir to Wachusett Mt. in the background. The first set of measurements occurred on 5 September 1991 under conditions of light winds from the east. A second set of measurements occurred on 11 September 1991 under conditions of stronger winds from the west. Strong Bragg spikes in clutter power spectra from small inland bodies of water at low but nonzero-Doppler velocities make these results interesting from multidisciplinary points of view, for example, in contexts of (a) the total clutter environment over land, (b) remote sensing, and (c) sea clutter.

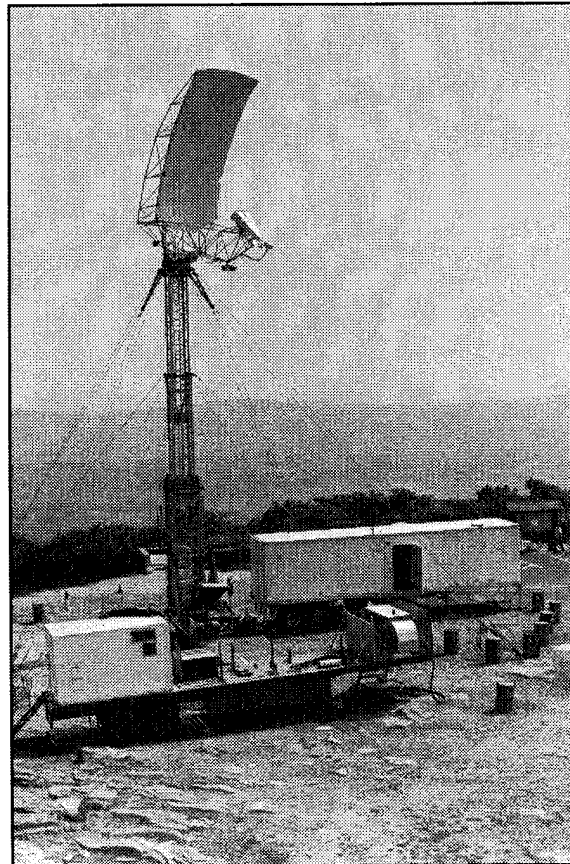


Figure 1. The LCE radar on Wachusett Mt.

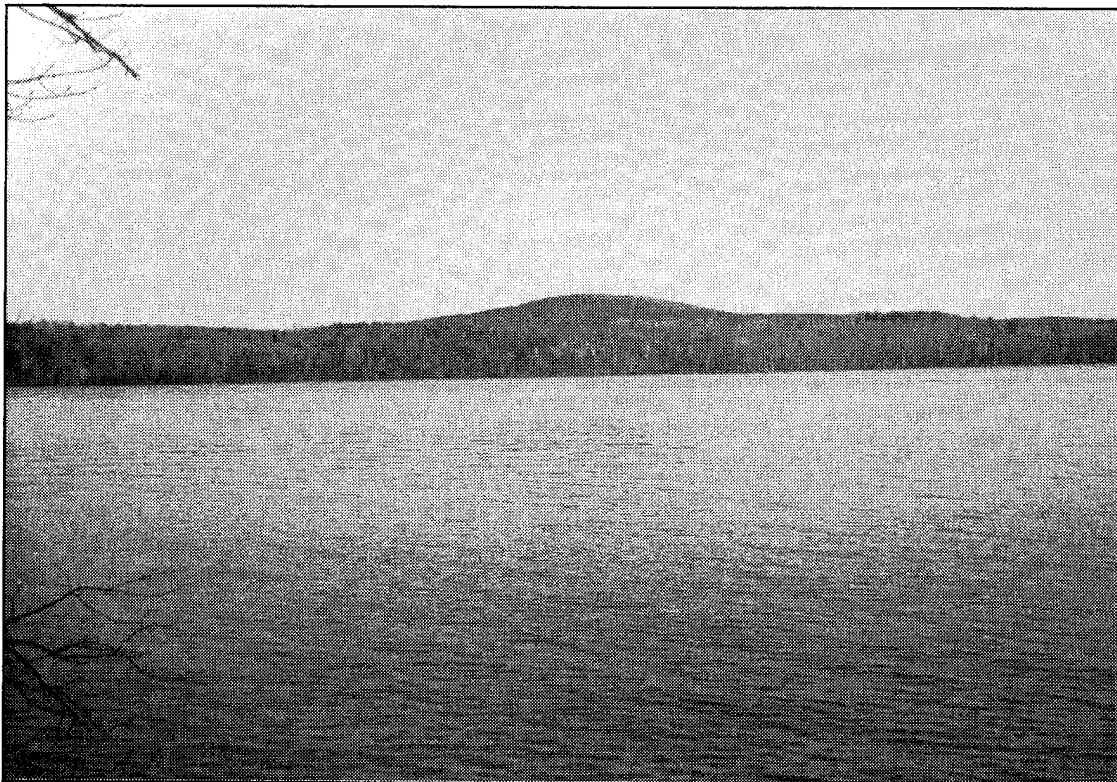


Figure 2. View from the west shore across Mare Meadow Reservoir east to Wachusett Mt. in the distance.

Bragg resonance occurs from successive water waves spaced such that cophased contributions occur in the backscattered radar waves. The fundamental resonance occurs when the water waves are spaced at one-half the radar wavelength (one-half because a two-way radar transmission path is involved). The Doppler shift of the first or fundamental Bragg resonance is given by:

$$f_b = \pm \left[\frac{g \cos \theta}{\pi \lambda} \right]^{\frac{1}{2}} \quad (1)$$

where g is the acceleration due to earth's gravity ($g = 9.807 \text{ m/s}^2$), λ is the radar wavelength, and θ is the grazing angle [1]. Higher-order resonances can also occur in which secondary peaks appear to either side of the first-order spikes in sea clutter Doppler spectra [2]. The positions and amplitudes of the secondary peaks vary with water wave amplitude and direction [3]. Bragg scattering in sea clutter has been a subject of interest both at high (HF) and microwave frequencies. At HF, sharp Bragg resonances often occur in a highly developed way and can provide information about remote sea currents and waves [3]. At micro-

wave frequencies, Bragg resonances are often (but not always) obscured by advective motion of large-scale ocean swell [4]. Nevertheless, the development of theories to explain microwave sea return has been based on Bragg-scattering ideas that have received strong support from wave tank studies in which sharp Bragg resonances have been routinely observed from wind-generated waves [4,5]. Useful introductions to the literature on Bragg scattering in sea clutter are provided in Long [1] and Tucker [2].

The main purpose of the LCE radar was to measure and characterize spectral spreading due to intrinsic motion of windblown vegetation in radar ground clutter. However, one of the three measurement radials selected at Wachusett Mt., primarily for recording backscatter from windblown trees, was also secondarily selected because it provided LCE visibility to the surface of Mare Meadow Reservoir. The principal subject of this report is the Bragg resonance observed in the backscatter from the reservoir surface. Several examples of clutter spectra from windblown trees are also included and compared with Bragg resonant water clutter spectra. The main LCE findings concerning the general characterization of Doppler spreading in clutter returns from windblown vegetation are presented elsewhere [6,7].

2. LCE RADAR INSTRUMENTATION

The LCE radar was a major L-band-only upgrade of the Lincoln Laboratory Phase One five-frequency ground clutter measurement radar [8,9]. A primary design objective of the LCE radar was to achieve low phase noise such that the low-frequency Doppler components of windblown clutter could be measured to levels ≈ 80 dB below the dc or stationary component of the clutter at zero-Doppler. This objective was met by using a combination of low phase-noise local oscillators (viz., Hewlett-Packard models 8662A and 8663A) locked to a common source, a low phase-noise transmitter, and system clocks with low jitter. The transmitter used two planar triodes (viz., Eimac Y-793F) in a grounded-grid amplifier configuration providing inherently low noise sensitivity [10].

A number of important system parameters of the LCE radar are shown in Table 1. The radar receiver achieved high dynamic range through careful gain distribution and proper choice of mixers and amplifiers, with particular attention paid to maintaining overall system linearity. The two channels of the in-phase and quadrature (I/Q) detector, which operated at a receiver IF of 3 GHz, were balanced to within approximately 0.1 dB in amplitude and 1 degree of phase. This balance provided approximately 40 dB of image rejection. The receiver I/Q outputs were digitized by 14-bit analog-to-digital (A/D) converters chosen for their linearity and speed (i.e., maximum clock speed = 10 MHz). The dc bias was temperature-regulated to approximately 100- μ V variation (i.e., to less than the least-significant bit of the A/D converter). The radar receiver, exciter, and control system were fabricated by System Planning Corporation, Arlington, Virginia, based on the design of their Mark IV instrumentation radar for measuring radar cross section (RCS). The data recording system was fabricated by Echotek Corporation of Huntsville, Alabama.

LCE clutter data were acquired with a stationary antenna over 70-s data recording intervals called experiments. All the experiment results shown in this report were obtained utilizing the following parameters: 1230-MHz radar frequency, 500-Hz pulse repetition frequency (PRF), 1- μ s pulsewidth, 2-MHz sampling (i.e., 75-m range gate spacing), 70 s of data recording (35,000 pulses), 80 samples per pulse repetition interval (PRI) (i.e., 80 range gates total), and 6-km total range swath (e.g., 2.8 to 8.8 km). Clutter experiments were usually taken in groups of six covering the various LCE polarization combinations. These six standard sequential experiments were HH, VV, HV, VH, HH, VV (i.e., HH and VV were repeated). HV means transmit horizontal polarization, receive vertical polarization, and so on.

All the clutter power spectra shown in this report were computed directly as fast Fourier transforms (FFTs) of the sampled temporal pulse-by-pulse return, including the dc component. The spectral power density is displayed in decibels of received power with respect to 1 W (dBW) per Doppler velocity resolution cell Δv at the LCE antenna terminal versus Doppler velocity v in meters per second (m/s) on linear and/or log velocity scales. In LCE data reduction, each temporal record of 30,720 pulses (first 61.44 s of each 70-s experiment) was divided into contiguous groups of 5120 samples, a 1024-point complex FFT was generated for each group by utilizing every fifth pulse, and the amplitudes of the resultant set of FFTs were arithmetically averaged together in each Doppler cell to provide the spectrum illustrated. Thus each LCE spectrum shown is the result of averaging 6 individual spectra (each from a 1024-point FFT) from an overall record of 1.024-min duration, utilizing an effective 10-ms PRI and an effective 100-Hz PRF. The duration of temporal backscatter data processed for each FFT was 10.24 s. In generating each LCE spectrum, a 4-Term Blackman-Harris window function was utilized with highest sidelobe level at -92 dB [11]. The Doppler velocity resolution cell Δv is wider than the sampling interval by a factor equal to the equivalent noise bandwidth (ENBW) of the window function. Thus $\Delta v = (\lambda/2) \cdot (\text{PRF}/1024) \cdot \text{ENBW}$. For the 4-Term Blackman-Harris window utilized here with 1024-point processing, $\text{ENBW} = 2.004$ [11]

TABLE 1
LCE Radar System Parameters

Parameter	Specification
Frequency	1230 MHz
Tower height	50 ft
Pedestal	$\pm 15^\circ$ El over $\pm 180^\circ$ Az
Antenna	
Type	Offset fed parabolic section
Gain	31 dBi
Beamwidth	3° El; 6° Az
Peak sidelobes	-17-dB El; -22-dB Az
Polarization	HH, VV, HV, VH (switch selectable)
Peak power	8 kW
PRF	500 Hz
Pulsewidth	1 μ s
Waveform	Uncoded CW pulse
Phase noise	-80 dBc at frequencies ≥ 50 Hz in a 10-Hz bandwidth
Spurious signals	Power line related spurs -72 dBc or lower
Receiver noise figure	2 dB
A/D converter	
No. of bits	14
Sampling rate	2 MHz
I/Q balance	Supports -40-dB image rejection
Data recording	
No. of samples	80/PRI
Sampling rate	2 MHz

Doppler frequency f_d in Hertz and radial Doppler velocity v in meters per second are fundamentally related as $f_d = 2v/\lambda$, where λ is radar wavelength in meters. Because of this fundamental linear relationship between Doppler frequency and scatterer radial velocity, the Doppler frequency extent of measured clutter spectra from windblown vegetation usually scales approximately linearly with radar frequency, whereas the Doppler velocity extent from windblown vegetation remains largely invariant with radar frequency [6,7]. Plotting measured clutter spectra from windblown vegetation utilizing a Doppler velocity abscissa as opposed to the more commonly used Doppler frequency abscissa allows direct comparison of spectral shape and extent at different radar frequencies with the linear scaling factor normalized out. Note that whereas fundamentally, f_d varies as λ^{-1} , Equation (1) indicates that the Doppler shift of Bragg resonance varies as $\lambda^{-0.5}$. As a result, the positions of the Bragg resonant lines in inland water Doppler velocity clutter spectra (as opposed to frequency spectra) are not invariant with radar frequency but vary as $\lambda^{+0.5}$. Although the Doppler velocity interval of tree spectra is itself largely invariant with radar frequency, the relative position (i.e., Doppler velocity shift) of the inland water Bragg spike within this interval varies inversely with the square root of the radar frequency.

There were two LCE clutter measurement sites. The first was Wachusett Mt., where backscatter data were recorded from a dense tree canopy typical of the eastern mixed forest. The second was a Nevada site where backscatter data were recorded from sparse scrub vegetation typical of the western desert. Figure 3 shows two LCE-measured clutter spectra, one from each measurement site, which are among the narrowest and widest of all those examined. The narrow spectrum in Figure 3(a) is from a desert cell at the Nevada site. For this measurement, the wind conditions were very calm, resulting in no discernible motion of the sparse desert scrub vegetation on the desert floor within the measurement cell. As a result, this spectrum essentially contains only dc power from the stationary desert floor. This dc spectral component at zero-Doppler velocity is very narrow. In fact, its width is just the limit of spectral resolution provided by the Blackman-Harris window function as used here in 1024-point FFT processing of 10.24 s temporal data records. The zero-Doppler return maintains this limiting window function resolution over the full 80 dB of spectral dynamic range shown in Figure 3(a). The window function sidelobes occur below the system noise level of -80 dB. System stability is such that no internally caused spectral contaminants occur outside the steady signal frequency characteristic of the window function down to the system noise level. Eighty decibels of spectral dynamic range for making clutter measurements is much greater than was previously available in most earlier measurements of ground clutter spectra [12-14].¹

The wide spectrum in Figure 3(b) is from a forested cell at the Wachusett Mt. site under windy conditions (15 to 20 mph). The rate of decay of spectral power in this spectrum with increasing Doppler velocity is very nearly exponential, as indicated by the good fit of the data to the straight line drawn through the right side of the spectrum. The maximum spectral extent in Figure 3(b) is ≈ 3 m/s at a spectral power level 67 dB below the maximum power level in the spectrum. Occasional earlier reports² of spectral extent from windblown trees to much greater Doppler velocities than ≈ 3 m/s have never been corroborated by any results from the extensive Lincoln Laboratory data base of LCE and Phase One windblown clutter spectral measurements. The general findings from this data base concerning spectral shape and extent from windblown vegetation are much more completely discussed elsewhere [6,7].

¹Billingsley [7] reviews many early measurements of ground clutter spectra.

²For example, Simkins et al. [14] report maximum measured spectral extent of 5.8 m/s at a spectral power level 40 dB down from the peak zero-Doppler level, for heavily wooded valleys under 10- to 20-kn winds. These results were subsequently modeled as an $n = 3$ power law that was extrapolated to a Doppler velocity of 30 m/s, 60 dB down.

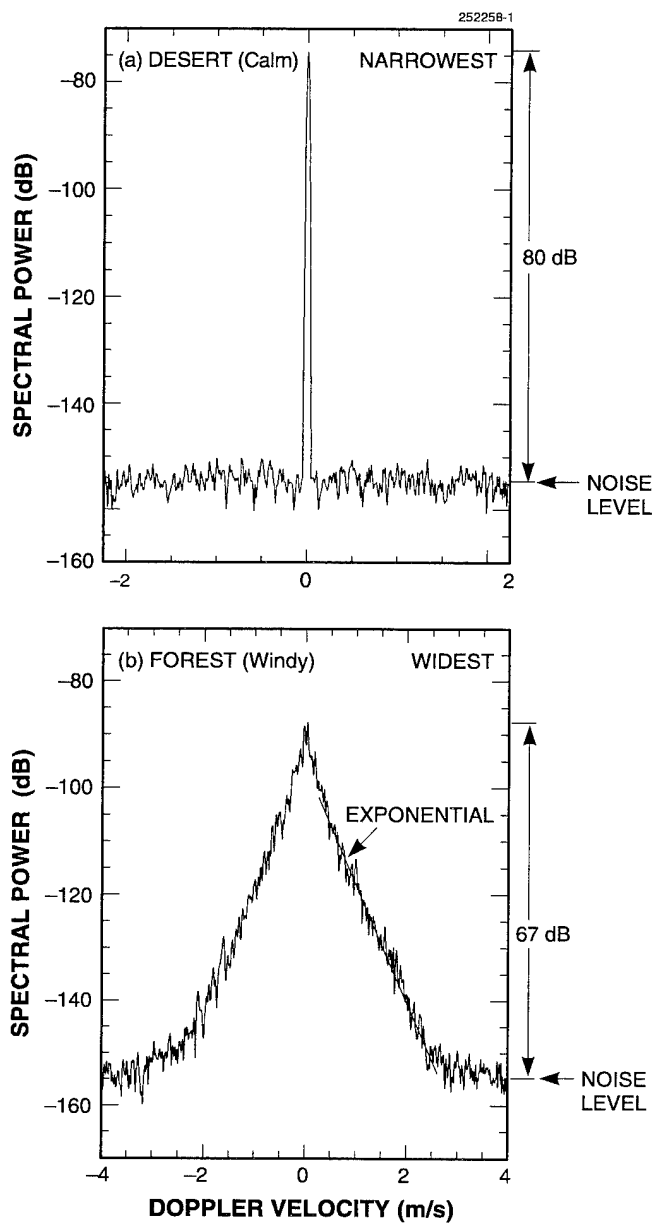


Figure 3. Narrowest and widest LCE-measured clutter spectra. (a) Nevada desert vegetation, still air, range gate 33 (4.4 km), HH-pol., 9 December 1991; (b) Massachusetts forest vegetation, windy, range gate 53 (7.9 km), VV-pol., 11 September 1991.

3. LCE-MEASURED BRAGG RESONANCE RESULTS

3.1 LIGHT WIND CONDITIONS

Figure 4 shows a clutter spectrum measured by the LCE radar from the surface of Mare Meadow Reservoir on 5 September 1991. Polarization is VV, for which water returns are strongest. Figure 4(a) shows the spectrum on a linear Doppler velocity x -axis. Figures 4(b) and 4(c) show the right and left sides of the spectrum, respectively, on log Doppler velocity axes. This spectrum illustrates a well-developed Bragg resonance phenomenon with the following features:

- A clutter spectrum from the slightly wavy surface of Mare Meadow Reservoir of approximate bell shape, but with an overall displacement to the left of zero-Doppler velocity in the direction of negative Doppler velocities. Such a spectrum is typical of sea clutter spectra with the radar looking downwind. In this measurement, winds³ were light (6 to 11 mph), generally from east to northeast, and the radar was looking west along $Az = 294^\circ$, so the radar was looking obliquely downwind at water waves that were receding.⁴ Thus the expectation is of a negatively shifted Doppler spectrum, as observed in Figure 4.
- Two sharp narrow peaks or spikes nearly symmetrically positioned to either side of zero Doppler and rising 20 to 25 dB above the general level of the otherwise approximately bell-shaped clutter spectrum from Mare Meadow Reservoir. These spikes occur very nearly at the Bragg resonant frequencies given by Equation (1) to be $f_b = \pm 3.57$ Hz for the LCE L-band radar frequency of 1230 MHz (or, equivalently, at Doppler velocities given to be ± 0.436 m/s). Thus these dominant double spikes offset from zero Doppler indicate the existence of a strong Bragg resonance in the backscattered temporal record from the inland water cell from which this spectrum was produced. The required wavelength of water waves to support this Bragg resonance is 4.8 in. The existence of a significant 4.8-in wavelength component within the spectrum of water waves existing under the measurement conditions of light winds working over a fetch of several hundred meters pertaining to these data is highly plausible.
- Bragg splitting. Double peaks are not always observed in Bragg backscattering from water. When they do occur, the phenomenon is referred to as "Bragg splitting" [4]. In Figure 4, the exact frequencies at which the two first-order Bragg lines occur are -3.81 and $+3.42$ Hz (i.e., -0.465 and $+0.417$ m/s). That is, the first-order lines in this figure are not exactly symmetrically positioned to either side of zero Doppler. First-order Bragg lines

³For LCE clutter measurements at Wachusett Mt., wind conditions were measured at 10-s update intervals with an anemometer stationed on top of a 75-ft tower in a treed clutter cell at $Az = 166^\circ$, range = 7.42 km. This cell is 10.3 km from the Mare Meadow Reservoir clutter measurement cell. Precise wind conditions in the Mare Meadow Reservoir cell are not available.

⁴The average wind direction recorded at the 10.3-km distant anemometer station for this experiment was from the northeast at 42° . The radar look direction with respect to wind direction was 108° . These and similar data from other experiments indicate that wind direction at Mare Meadow Reservoir on 5 September 1991 was generally from northeast to east such that the radar was looking obliquely downwind with corresponding negative Doppler shifts in the reservoir spectra.

that are not exactly symmetrically positioned at their predicted frequencies to either side of zero Doppler indicate a surface current such that the water waves causing the first-order scattering are superimposed on a water surface that is physically moving [3]. In Figure 4, the offset of the two first-order Bragg lines from symmetrical positioning is -0.024 m/s, indicating the existence of a small surface current away from the radar due to the slightly downwind radar look direction pertaining to these data. The total separation of the two first-order Bragg lines in the figure is 7.23 Hz (i.e., 0.881 m/s), compared with 7.15 Hz (i.e., 0.872 m/s) as predicted by Equation (1), which represents very close agreement between theory and measurement for this phenomenon. In addition to resonance very nearly at the expected Bragg frequency, Bragg splitting (two lines), and an offset due to surface current, the data of Figure 4 also show strong evidence of higher-order Bragg resonances to either side of the first-order Bragg lines, much as indicated in the examples of previously published HF sea clutter spectra shown later in this report. Thus the details of the spectrum in the figure corroborate the existence of a highly developed Bragg resonance phenomenon in these data.

- The total spectral power of the inland water spectrum of Figure 4 is -88 dBW at the antenna terminals. Most of this power is concentrated in the left-hand Bragg line offset from zero Doppler and is within 10 dB of spectral power levels found in some neighboring LCE ground clutter cells. The -88 -dBW level corresponds to a backscattering clutter coefficient $\sigma^{\circ} = -48$ dB, utilizing the parameters of Table 1 in the radar range equation, where σ° is defined to be RCS per unit surface area in the resolution cell, including propagation effects. When the Phase One radar was on Wachusett Mt. in August 1984, its measurements also included backscatter data from the Mare Meadow Reservoir cells in survey (i.e., scan) mode, which (for L-band, VV-pol., 15 -m pulse length) yielded $\sigma^{\circ} = -50$ dB, in close agreement with the 5 September 1991 LCE result. Such σ° levels from inland bodies of water, in which (as evidenced by the data of Figure 4) most of the power is concentrated in nonzero-Doppler Bragg lines, are not inconsequential within the overall context of ground clutter, even though the ground clutter σ° is generally much higher (e.g., along the 294° radial at Wachusett Mt., L-band ground clutter σ° ranges from -15 to -40 dB).

Figure 5 repeats the spectrum for range gate 20 shown in Figure 4(a) and includes an estimate of the amount of power included in this spectrum from adjacent forested ground (as opposed to water) entering through the antenna sidelobes. For range gate 20, the cross-range one-way beam extent of 416 m is entirely contained on the surface of Mare Meadow Reservoir; further out in cross-range, the forested shoreline is coincidentally intercepted in both cross-range directions very nearly in another one-half beamwidth (i.e., at ± 416 m cross-range from boresight). Ground clutter power thus enters the spectrum of range gate 20 from the forested shoreline and beyond through the antenna sidelobes. In Figure 5, the small peak in the spectrum at zero-Doppler velocity is due to ground clutter entering through the antenna sidelobes. The dotted line estimates the spectral shape of this small amount of corrupting ground clutter power. The power level of this ground clutter estimate decreases very rapidly to either side of zero Doppler. Thus only very near zero-Doppler velocity is the inland water spectrum even slightly corrupted (i.e., the small peak at zero Doppler) by ground clutter leakage through antenna sidelobes. The shape of the dotted ground clutter contribution in Figure 5 mirrors the narrow shapes of measured ground clutter spectra in nearby cells.

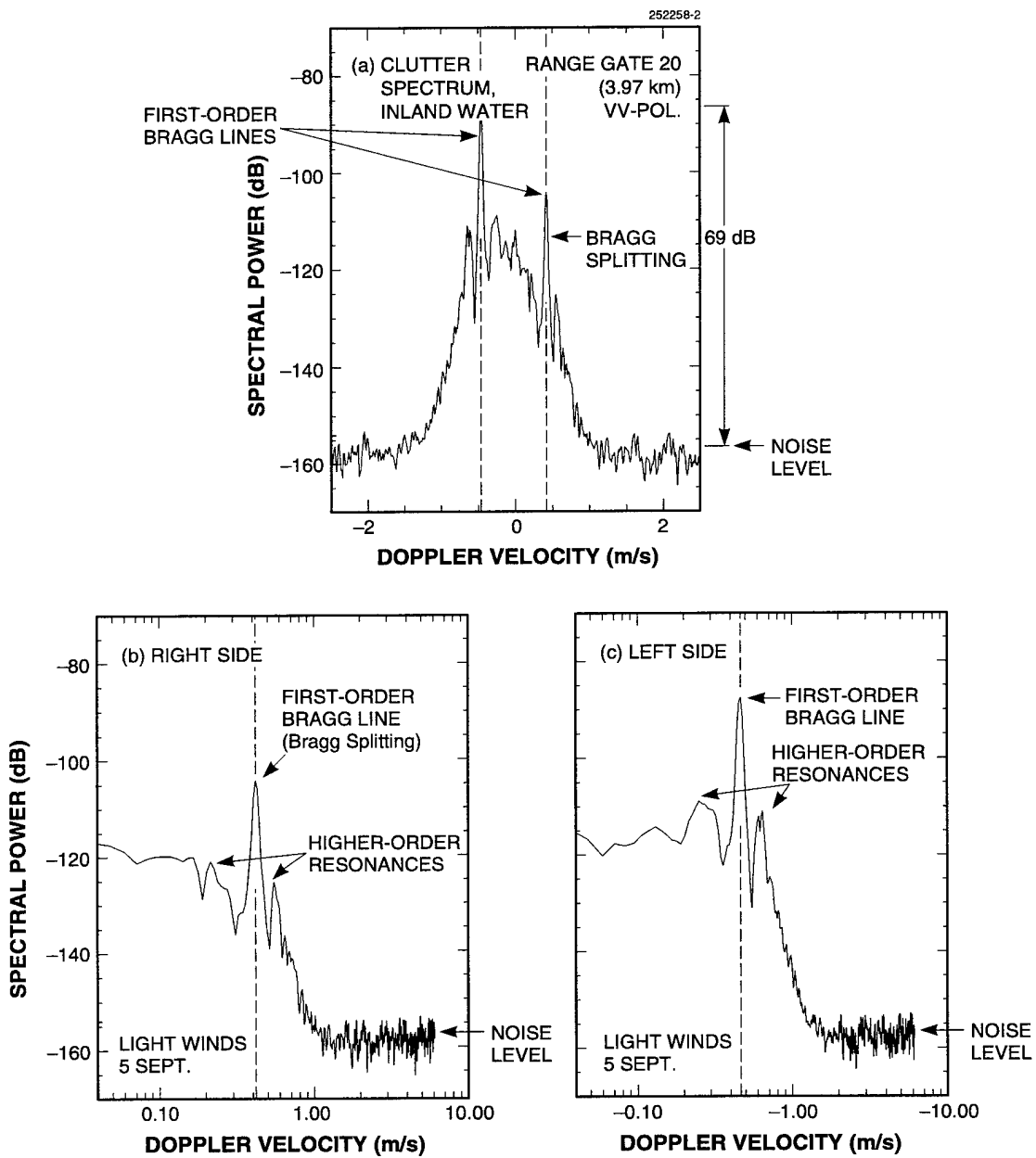


Figure 4. LCE-measured clutter power spectrum from the windblown fresh-water surface of Mare Meadow Reservoir showing strong Bragg resonances. Measurements performed on 5 September 1991, a light-winds day with the radar looking obliquely downwind; VV-pol., range gate 20 (3.97 km), (a) linear Doppler velocity axis, (b) log Doppler velocity axis, right side, and (c) log axis, left side.

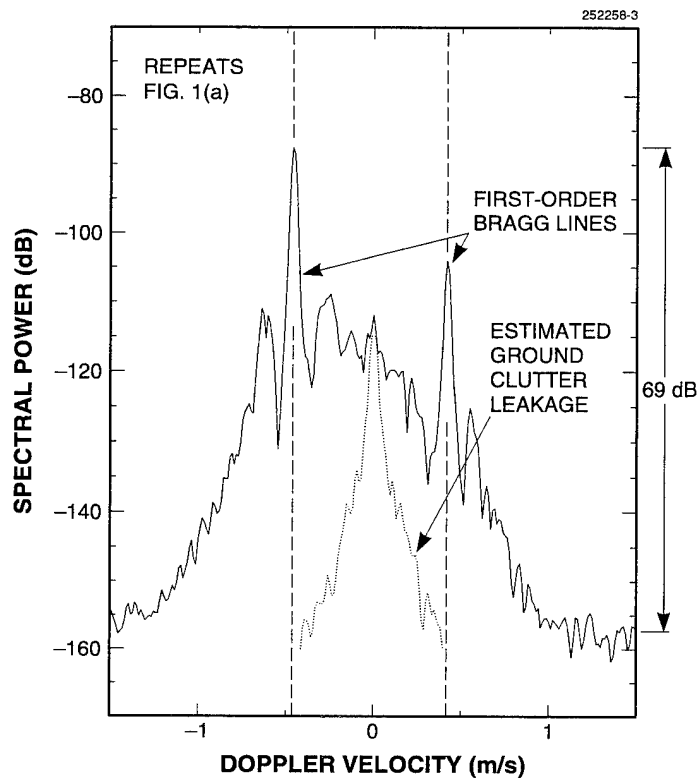


Figure 5. Figure 1(a) is repeated; estimated ground clutter leakage through antenna sidelobes shown as dotted line.

Figure 6(a) shows the I-channel temporal record from the inland water clutter cell from which the spectrum of Figure 4 was produced. (The Q-channel record was similar.) This temporal record comprises 35,000 pulses over a 70-s duration. The relatively rapid oscillation in this record is at the Bragg resonant frequency of ≈ 3.8 Hz, which is the dominant characteristic. Also visible in Figure 6(a) is a slower modulation. Note that this temporal record from water is largely symmetrical about zero amplitude, indicating relatively little dc or zero-Doppler component as confirmed in Figure 4.

In contrast to Figure 6(a), which is a temporal record of backscatter from water, Figure 6(b) is a temporal record of backscatter from trees. Both records were measured simultaneously (i.e., same experiment). The temporal record of Figure 6(b) comes from a range cell 375-m closer to the radar than the water cell of Figure 6(a). This closer range cell is treed on the near shoreline of Mare Meadow Reservoir. Figure 6(b) shows the amplitude of the Q-channel (the amplitude of the I-channel was similar). The temporal record from trees in Figure 6(b) is very different from that of water in Figure 6(a) in that the temporal record from trees is not dominated by a rapid Bragg resonance oscillation, and furthermore, it is significantly displaced below zero amplitude, indicating a strong dc or zero-Doppler component. The tree clutter spectrum derived from the temporal record of Figure 6(b) is shown in Figure 7, range gate 15.

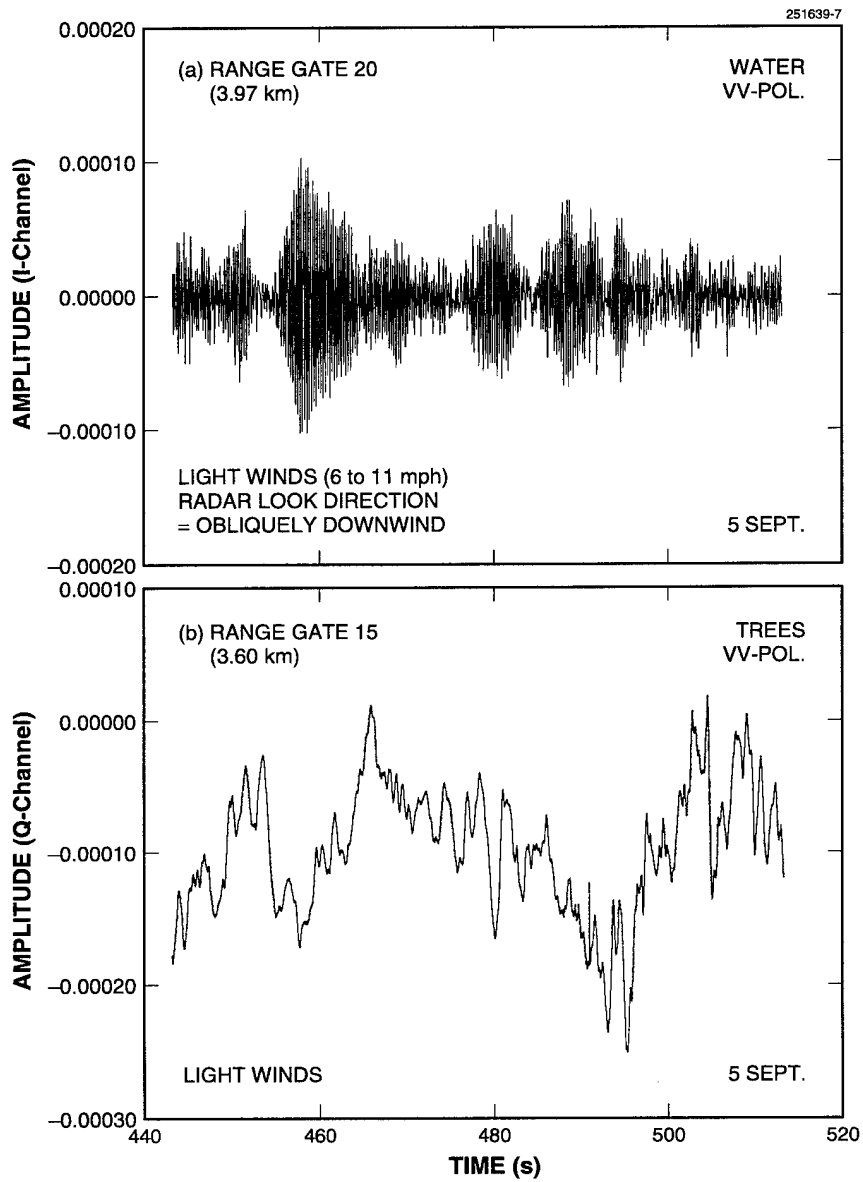


Figure 6. LCE-measured clutter amplitude temporal records; 5 September, VV-pol. (a) range gate 20 (3.97 km), water (Mare Meadow Reservoir), and (b) gate 15 (3.60 km), trees (near shore).

3.2 ADDITIONAL RANGE GATES

Figure 7 shows how the measured clutter spectra vary with increasing range across Mare Meadow Reservoir for the same experiment as illustrated in Figure 4. Results are shown for three range gate positions—15, 19, and 21. For each, the left side (i.e., negative Doppler velocities) of the spectrum is shown on a log Doppler velocity axis. The range resolution of the LCE radar is 150 m, but the sampling interval in range is 75 m, so it is necessary to increment gate position by two to obtain independent results. Bragg resonance from the reservoir surface was observable over seven contiguous reservoir range gates—16 through 22.

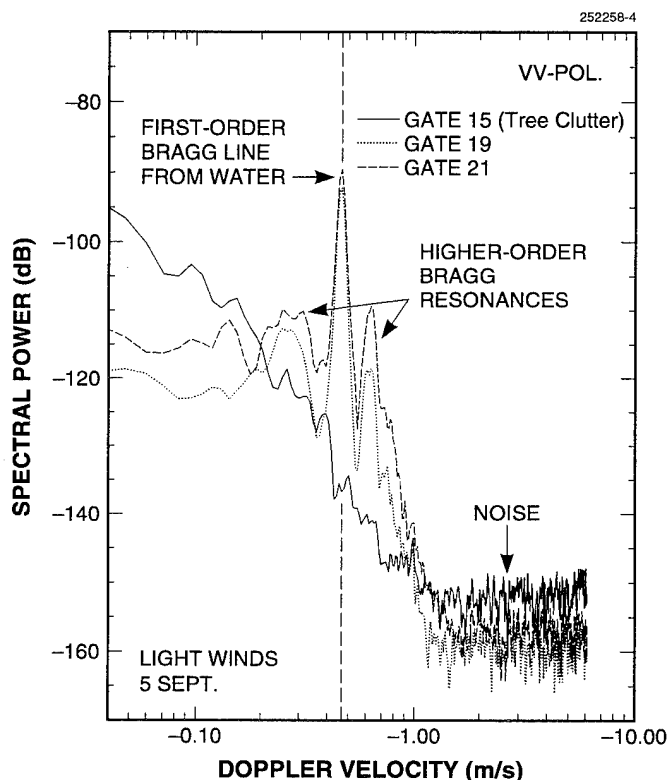


Figure 7. LCE-measured clutter power spectra showing variations with range as range gate position traverses Mare Meadow Reservoir; 5 September, VV-pol., gate 15 (3.60 km), trees; gate 19 (3.90 km), water; gate 21 (4.05 km), water.

Figure 7 includes the forest clutter spectrum in gate 15 at 3.60-km range from along the near shoreline of Mare Meadow Reservoir. The temporal record from which this spectrum was derived is shown in Figure 6(b). The forest surrounding Mare Meadow Reservoir is a typical eastern mixed hardwood forest (e.g., oak, maple, beech) with occasional occurrences of conifers (e.g., hemlock, pine), all rising to heights generally of 50 or 60 ft. In these August and September LCE measurements from Wachusett Mt., leaves were still on deciduous trees. Under the light, 6- to 11-mph winds of the 5 September experiment (from which results are

shown in Figure 7), the tree clutter spectrum of gate 15 is relatively narrow, certainly much narrower than the widest tree clutter spectrum measured by the LCE radar shown in Figure 3(b).

Figure 7 also includes water clutter spectra from gates 19 and 21, which bracket those from gate 20 shown in Figure 4. Gates 19 and 21 show inland water clutter power spectra very similar to those of gate 20, containing nearly (gate 19) or, indeed, as much (gate 21) total clutter power from the water surface as that of gate 20, with essentially as full-blown Bragg resonance phenomena as that of gate 20. For $|v| \leq \approx 0.1$ m/s, the data from gates 19 and 21 become corrupted by forested ground clutter near zero Doppler leaking through antenna sidelobes. Figure 7 does not show the clutter spectrum from gate 17 at 3.75-km range. This range gate was largely in shadow, resulting in relatively little total clutter power in the spectrum. Trees along the near shoreline and on a preceding hill masked the water surface of Mare Meadow Reservoir to the LCE radar to an approximate range of 3.8 km, or 200 m out from the near shore. Some reduced tree clutter power entered gate 17 through the azimuth sidelobes from the near shoreline. First-order Bragg resonance lines were observed in the spectrum from gate 17 at low levels superimposed on the reduced-gain tree clutter spectrum. Presumably, some small portions of the water surface were visible between the preceding masking treetops in gate 17, although some foliage penetration through and/or diffraction over the treetops may also have occurred. Thus the existence of Bragg resonance in the backscatter from the surface of Mare Meadow Reservoir is not a singular or extraordinary event existing in only one gate, but a robust phenomenon existing in all gates of this experiment in which some water surface is visible.

The differences between inland water clutter spectra and tree clutter spectra in the same neighborhood are important to understand if signal processing algorithms for clutter-limited target detection are to perform adequately in such neighborhoods. It is very evident in Figure 7 that for $|v| > \sim 0.2$ m/s, water clutter power in gates 19 and 21 exceeds tree clutter power in gate 15 (plotted as the solid line) by large amounts. The shape of the tree clutter spectrum of gate 15 in Figure 7 is similar to the shapes of tree clutter spectra in many cells in the general region surrounding the reservoir. At dc or zero Doppler, the gate 15 tree clutter spectrum shown in Figure 7 is ≈ 10 dB stronger than the peak levels of the dominant Bragg lines in the water clutter spectra of gates 19 through 21, and furthermore, the total spectral power of the gate 15 tree clutter spectrum exceeds that of the gates 19 through 21 water clutter spectra by ≈ 10 dB. However, at the -3.8 -Hz resonant frequency of the dominant Bragg line, the gates 19 through 21 water clutter spectral power levels exceed the time-coincident gate 15 tree clutter spectral power level by 40 to 45 dB, and even exceed—by 17 dB—the maximum tree clutter spectral power ever measured by the LCE radar at ± 3.8 Hz, as shown in Figure 3(b). That is, at low but nonzero Bragg resonant frequencies, typically encountered levels of water clutter spectral power at VV-pol. can exceed neighboring land clutter spectral power levels at these frequencies by large amounts.

If total ac spectral power is normalized to unity in both the tree and water spectra of Figures 4 and 7 to focus on spectral shape on an equivalent ac power basis and keep separate the effects on spectral power level of differing σ^0 and ratio of dc/ac power in tree and water cells, the net effect is that the gate 15 tree spectrum drops by 7.4, 2.8, and 3.6 dB, respectively, compared with the water spectra of gates 19, 20, and 21. This matter is further discussed in Section 4.2.

3.3 PERSISTENCE WITH TIME AND POLARIZATION

To this point, only one 5 September LCE clutter experiment has been discussed. It has been shown that Bragg resonance occurs in all range gates of this experiment that provide any visibility of the surface of Mare Meadow Reservoir. That is, the resonant phenomenon is observed to be spatially extensive over seven range gates of 75-m spacing during the 70-s duration of this experiment. It is now shown that the Bragg resonance phenomenon of 5 September also persists in time as well as exists for all polarization states throughout the 15-min LCE data acquisition period that occurred for $Az = 294^\circ$ on 5 September. Thus Figure 8 shows spectra from the first four of the six different experiments spanning this 15-min time period, each from range gate 20, which provides the most ground-clutter-free measurement of the inland water surface of Mare Meadow Reservoir. In acquisition time order, the polarization states for which results are shown are VV, HH, HV, VH. Note that the VV-pol. spectrum in Figure 8 repeats that shown in Figure 4; the other three spectra in Figure 8 are different experiments recorded sequentially after the first at several-minute intervals.⁵ As in Figure 7, Figure 8 shows the left side of each spectrum on a log Doppler velocity axis.

The inland water clutter spectrum in Figure 8 at VV-pol. from range gate 20 on Mare Meadow Reservoir repeats that of Figure 4. Figure 8 also shows the corresponding spectrum at HH-pol. from the same water gate from data acquired 2 min later—the most striking feature is the very large reduction in the backscattered power from the water surface in this spectrum, compared with the corresponding power at VV-pol. In fact, the only evidence of backscattered power from the water surface at HH-pol. in Figure 8 is in the first- and higher-order Bragg resonances that are still clearly apparent. The spectral power for $|v| < \approx 0.2$ m/s in the HH-pol. spectrum is forested ground clutter leakage entering through the azimuth sidelobes, which is also a good estimate of the amount of ground clutter power existing at VV-pol., since differences between forested ground clutter spectra of VV- and HH-pol. are relatively minor. The power levels in the backscattered power from the water in gate 20 are 30 to 40 dB weaker at HH- than at VV-pol.; 30 dB as measured by the differences in the levels of the higher-order Bragg resonant lines; 40 dB as measured by the differences in the levels of the first-order Bragg resonant lines. It is well known that sea clutter σ^0 levels are much weaker at HH- than at VV-pol. at L-band and lower frequencies. Thus the extreme difference in water clutter power levels observed between the VV- and HH-pol. spectra of Figure 8 is expected.

Water clutter spectra for gate 20 at HV- and VH-pol. are also shown in Figure 8. These cross-polarization spectra contain more water clutter power than the HH-pol. spectrum, although not as much as the VV-pol. First- and higher-order Bragg resonances are clearly observable in the cross-polarization spectra. Spectral power for $|v| < \approx 0.1$ m/s in these cross-polarization spectra, where it overlaps with that of the HH-pol. spectrum, is also forested ground clutter leakage. Measured by the differences in the levels of the higher-order Bragg resonant lines, the water clutter power levels at cross-polarization are about 20 dB stronger than at HH-pol. but about 15 dB weaker than at VV-pol.

⁵Each of the six 5 September experiments can be characterized by the mean and maximum wind speeds recorded by the 10.3 km distant anemometer at 10-s update intervals over the 70-s duration of each experiment, as 6/7, 7/9, 9/11, 6/8, 8/10, and 9/11 mph, respectively. The reservoir wind speeds throughout the total 15-min period covering all six experiments are characterized as roughly bounded by the minimum and maximum numbers, i.e., 6 to 11 mph.

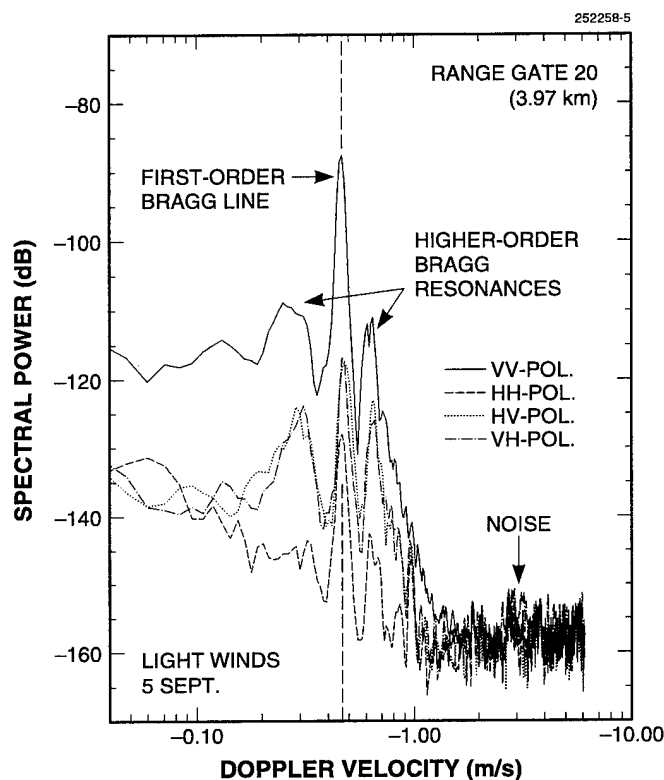


Figure 8. LCE-measured clutter power spectra from the surface of Mare Meadow Reservoir showing variations with VV-, HH-, HV-, and VH-pol., 5 September, range gate 20 (3.97 km).

Another interesting feature of the cross-polarization spectra (Figure 8) is that the levels of the higher-order resonant peaks are much nearer those of the first-order peaks (viz., within about 6 to 8 dB), compared with the copolarized spectra, where the first-order peaks are 15 to 25 dB stronger than the higher-order peaks. In the extensive literature of Bragg resonant scattering from sea surfaces, the positions and amplitudes of the second-order peaks with respect to the first-order spikes have been interpreted to provide information about sea state and wave direction [3,16]. In the upper HF region (6 to 30 MHz) at which remote sensing of ocean surfaces at great distances via ionospheric propagation can occur, the amplitudes of the first-order Bragg spikes are constant and insensitive to sea state. The reason is that the Bragg resonant water waves of 5 to 25 m in length (i.e., one-half the radar wavelength) in this region are nearly always present and developed to their maximum height as limited by breaking on the open ocean. In fact, the amplitudes of the first-order spikes can be used to calibrate the amplitudes of the higher-order peaks, which otherwise is a difficult task under ionospheric propagation. These matters are more fully discussed in Barrick et al. [3]. Such a complete set of results (as provided in Figure 8), showing fully developed Bragg resonance with respect to polarization (i.e., comparable results for four polarization states, viz., VV, HH, HV, VH) is not commonly available in the general literature of Bragg resonance in backscatter from water surfaces.

Figure 9 shows water clutter power spectra from gate 20 on Mare Meadow Reservoir for two experiments at VV-pol. in which the second experiment commenced 14 min 5 s after the first. The earlier spectrum in Figure 9 is the VV-pol. spectrum shown in Figures 4, 5, and 8. The degree of repeatability in the spectral results in Figure 9 is remarkable. Certainly, over this 15-min period of data acquisition, the neighborhood wind conditions as measured at the 10.3 km distant anemometer station were not invariant but undergoing the type of ephemeral variation typical of a day of light breezes. Thus as measured at 10-s update intervals over this period at the anemometer station, wind speeds ranged from 4 to 12 mph, and wind directions, although generally from the northeast, ranged from 18° to 105° . Presumably, similar variations were occurring in the breezes over Mare Meadow Reservoir with corresponding temporal variation in specific wave conditions. Thus the Bragg resonance observed in the LCE backscatter from Mare Meadow Reservoir on 5 September 1991 was a long-lived phenomenon not sensitive to the specificities of local wind variation from experiment to experiment over a 15-min period.

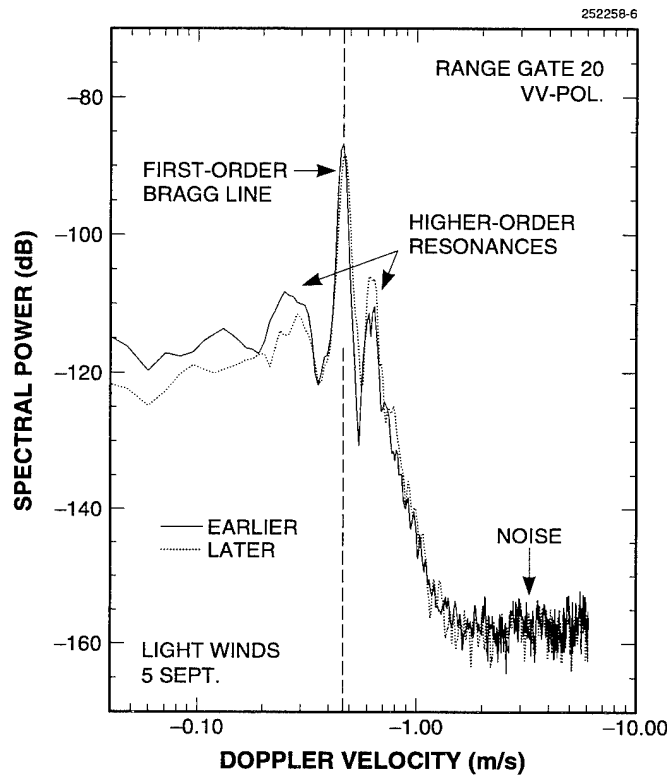


Figure 9. LCE-measured clutter power spectra from the surface of Mare Meadow Reservoir for two similar experiments showing variation with time of measurement; 5 September, range gate 20 (3.97 km), VV-pol. Later measurement performed 14 min 5 s after earlier measurement.

3.4 STRONGER WIND CONDITIONS

LCE measurements were obtained along the Mare Meadow Reservoir azimuth of 294° on two measurement days, 5 and 11 September. A full set of six experiments (i.e., VV, HH, HV, VH, VV, HH) was acquired on each day—over a 15-min period on 5 September when winds were light and from the east, and over a 22-min period on 11 September when winds were stronger and from the west.

Figure 10 shows the VV-pol., range gate 20 reservoir spectrum of 11 September displayed similarly to that of 5 September shown in Figure 4. Corresponding VV-pol., range gate 20 clutter spectra from the surface of Mare Meadow Reservoir for the light-winds day of 5 September and the windier day of 11 September are shown plotted together in Figure 11. On 11 September the winds not only were stronger than on 5 September but from the northwest (i.e., typically 310°) rather than the east such that the radar was looking almost directly (i.e., within 16° of) upwind. Indeed, Figure 11 shows the 11 September water clutter spectrum to be generally higher and wider than the 5 September spectrum due to the rougher water surface on 11 September, and displaced toward positive rather than negative Doppler velocities due to the reversed wind direction. Bragg resonance lines continue to be evident in the windier day spectrum of Figures 10 and 11, but rising only 6 to 8 dB above adjacent spectral levels, in contrast to the 20- to 25-dB Bragg rises in the light-winds day spectrum, partly due to the overall spectral level being higher on the windier day. Nevertheless, the absolute levels of the Bragg spikes on the windier day in these figures are 10 dB weaker than on the light-winds day (comparing dominant component with dominant and “split” component with “split”). Presumably, the rougher water surface on the windier day contained a less significant 4.8-in water wavelength component than on the light-winds day.

In Figure 11, the 11 September windier day spectrum is displaced significantly to the right of zero Doppler, compared with the slight displacement to the left of the 5 September light-winds day. At the -140 -dB power level in the spectra, the centroid of the light winds spectrum is at -0.1 m/s, whereas the centroid of the windier day spectrum is at $+0.38$ m/s. On the windier day, the radar is looking almost directly upwind at water waves that are advancing, in contrast to looking obliquely downwind on the light-winds day at water waves that are receding. That is, wave direction on the light winds day has a slight component away from the radar, whereas wave direction on the windier day has a stronger component toward the radar.

It is apparent in Figure 11 that the windier day Bragg lines are shifted slightly to the right of the light-winds day Bragg lines. The only reason that the Bragg lines do not exactly coincide with symmetrical positioning to either side of zero Doppler in these two measurements is that the surface currents on these two measurement days differ. That is, the Bragg line frequencies are unaffected by wind conditions (i.e., speed, direction) or wave conditions (i.e., amplitude, direction). As indicated earlier, the offset of the two first-order Bragg lines from symmetrical positioning in the 5 September spectrum in Figure 11 was -0.024 m/s, indicating the existence of a surface current with a small component away from the radar due to the slightly downwind radar look direction pertaining to these data. In comparison, the offset of the two first-order Bragg lines in the 11 September spectrum is $+0.071$ m/s, indicating the existence of a surface current with a larger component toward the radar due to the almost directly upwind radar look direction pertaining to these data. It is remarkable, however, that aside from these differences caused by differing surface currents on the two measurement days, the relative separation of the two first-order Bragg lines (i.e., the Doppler difference between the dominant and the split lines) is identical, equal to 7.23 Hz or 0.881 m/s, on both measurement days. That is, the Bragg spikes occur at -3.03 and at $+4.20$ Hz in the 11 September windier day spectrum of Figure 11 compared with their occurrence at -3.81 and at $+3.42$ Hz in the 5 September light-winds day spectrum.

The total power of the 11 September spectrum is 2.1 dB weaker than that of the 5 September spectrum, which leads to an 11 September clutter coefficient $\sigma^\circ = -50$ dB compared with the 5 September clutter coefficient $\sigma^\circ = -48$ dB. Sea clutter is generally expected to increase with sea state (i.e., wind speed), and as the radar look direction progresses from downwind to crosswind to upwind [17]. Except for the Bragg spikes, the windier day, upwind spectrum of 11 September in Figure 11 does appear to be generally higher and wider and thus to contain more backscattering power than the light-winds, crosswind-to-downwind spectrum of 5 September, as expected. However, the very strong Bragg spikes are enough to change the balance and result in the 5 September spectrum containing 2 dB more total spectral power than the 11 September spectrum. That is, variations in the degree of Bragg resonance encountered in a particular measurement may contribute to the large variability that exists in sea clutter measurements performed under nominally similar measurement situations and sea states [1,18]. Recall that the earlier Phase One Mare Meadow Reservoir result was also $\sigma^\circ = -50$ dB (L-band, VV-pol., 15-m pulse length), identical to the 11 September LCE result.

Figure 12 shows clutter amplitude temporal records from water (gate 20) and trees (gate 15) for the stronger winds day of 11 September, similar to the corresponding results shown in Figure 6 from the light-winds day of 5 September. The temporal record from water shown in Figure 12(a) is that from which the spectrum of Figure 10 was produced. Even though the Bragg spikes were 10 dB weaker on 11 September, they are still strong enough to cause a rapid Bragg oscillation in the water record of Figure 12(a) at the frequency of the dominant Bragg resonance line of 4.2 Hz in these data. There is not such a strong secondary modulation in Figure 12(a) as seen in Figure 6(a). Figure 12(a) shows a slightly lower overall amplitude envelope for the stronger winds day than does Figure 6(a) for the light-winds day. As in Figure 6(a), the water data in Figure 12(a) are largely symmetrical about zero amplitude, indicating relatively little dc or zero-Doppler component. In contrast, the tree data in Figure 12(b), as in Figure 6(b), are significantly displaced below zero amplitude, indicating a significant dc or zero-Doppler component.

Figure 13 shows windier day results from 11 September for the three range gates traversing Mare Meadow Reservoir in a manner paralleling the light-winds day results from 5 September shown in Figure 7. Appropriate to these upwind data, Figure 13 shows the right side of each spectrum on a log Doppler velocity axis. The gate 15 tree clutter spectrum was obtained from the temporal record shown in Figure 12(b). For $v > \sim 0.35$ m/s, the water clutter power in gates 19 and 21 of Figure 13 exceeds the tree clutter power in gate 15 (plotted as a solid line) even more clearly than in the 5 September data of Figure 7. For $v \leq \sim 0.2$ m/s, the data from gates 19 and 21 become corrupted by forested ground clutter near zero Doppler leaking through antenna sidelobes. Although the absolute levels of the Bragg spikes (both dominant and split) at VV-pol. on the windier day are 10 dB weaker than on the light-winds day as shown in Figure 11, the dominant Bragg spike at +4.2 Hz on the windier day is still 35 dB stronger than the time-coincident gate 15 tree clutter at +4.2 Hz as shown in Figure 13, and 10 dB stronger than the maximum tree clutter spectral power ever measured by the LCE radar at +4.2 Hz as shown in Figure 3(b). On the windier day, the difference between the peak zero-Doppler tree clutter power in gate 15 and the peak dominant Bragg line water clutter power in gate 20 was only 12 dB, compared with a corresponding 10-dB difference on the light-winds day. The small change in this difference from light-winds to windier day is partly due to the fact that the zero-Doppler tree clutter return was reduced by 3 dB on the windier day. On the windier day, the total power in the gate 20 water clutter spectrum of Figure 11 was 9 dB weaker than in the time-coincident gate 15 tree clutter spectrum of Figure 13 compared with 10 dB weaker on the light-winds day. On an equivalent total ac power basis, the windier day gate 15 tree spectrum of Figure 13 drops by 9.2, 3.1, and 5.2 dB, respectively, compared to the windier day water spectra of gates 19, 20, and 21.

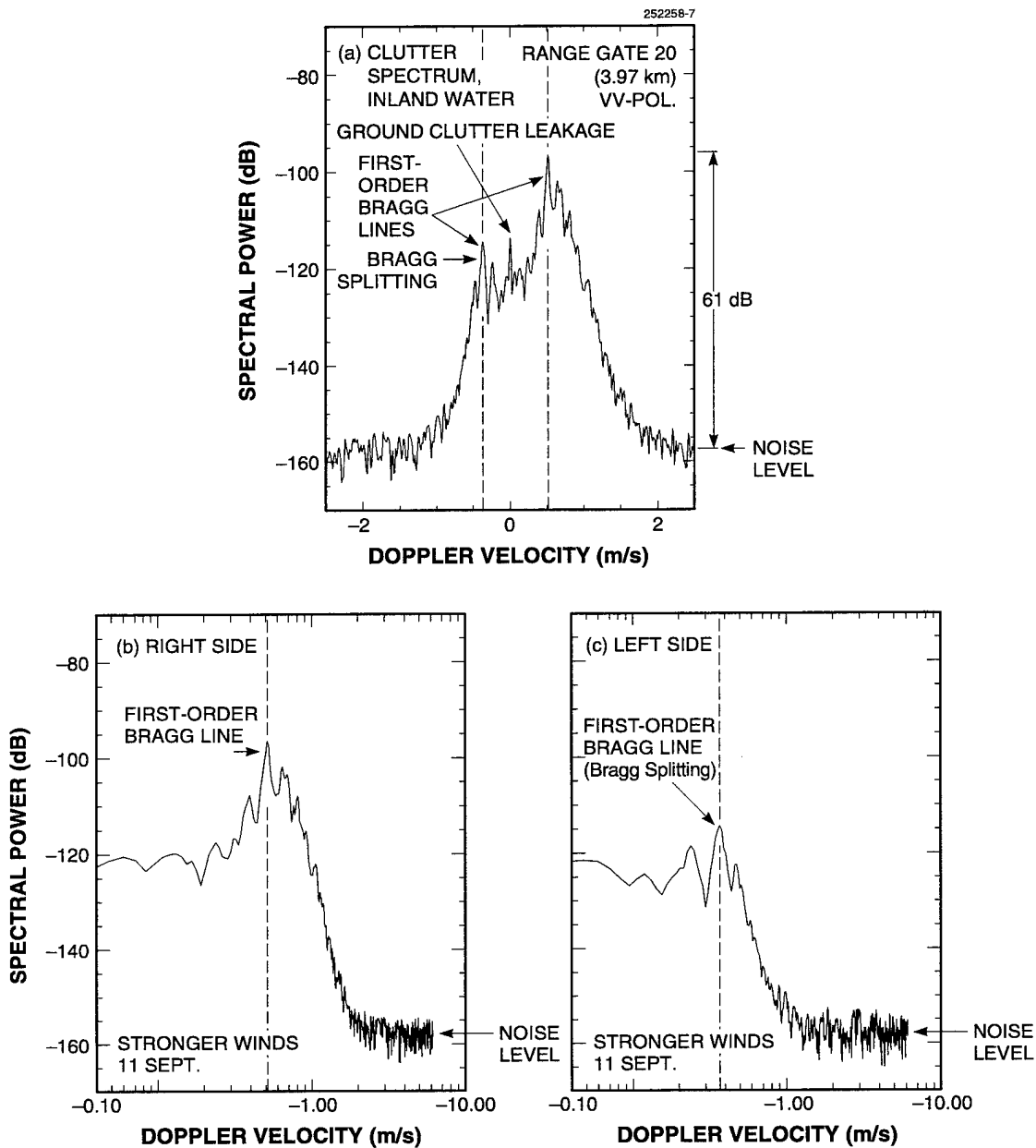


Figure 10. LCE-measured clutter power spectrum from the windblown fresh water surface of Mare Meadow Reservoir showing Bragg resonances. Measurements performed on 11 September, a day of stronger winds with the radar looking almost directly upwind, VV-pol., range gate 20 (3.97 km): (a) linear Doppler velocity axis, (b) log-Doppler velocity axis, right side, and (c) log-axis, left side.

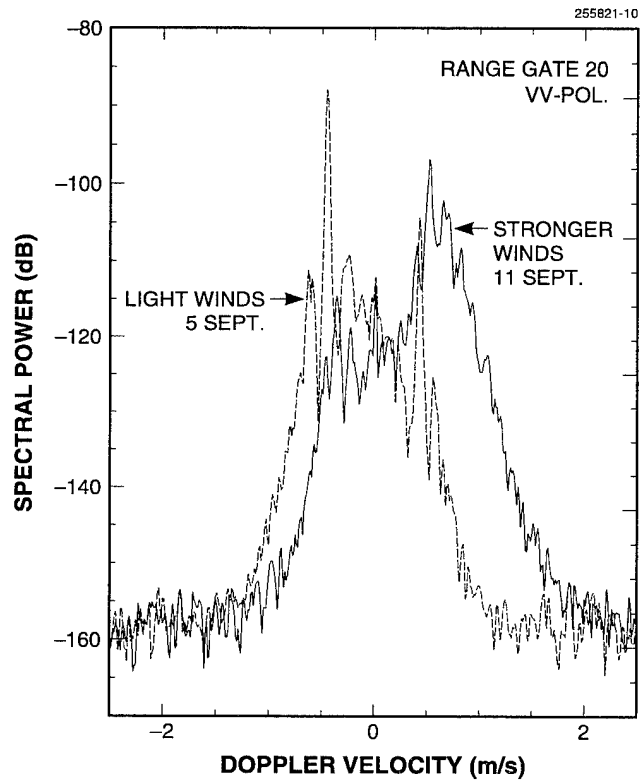


Figure 11. LCE-measured clutter power spectra from the surface of Mare Meadow Reservoir, showing variations with wind condition on two different days, 5 and 11 September: VV-pol., range gate 20 (3.97 km).

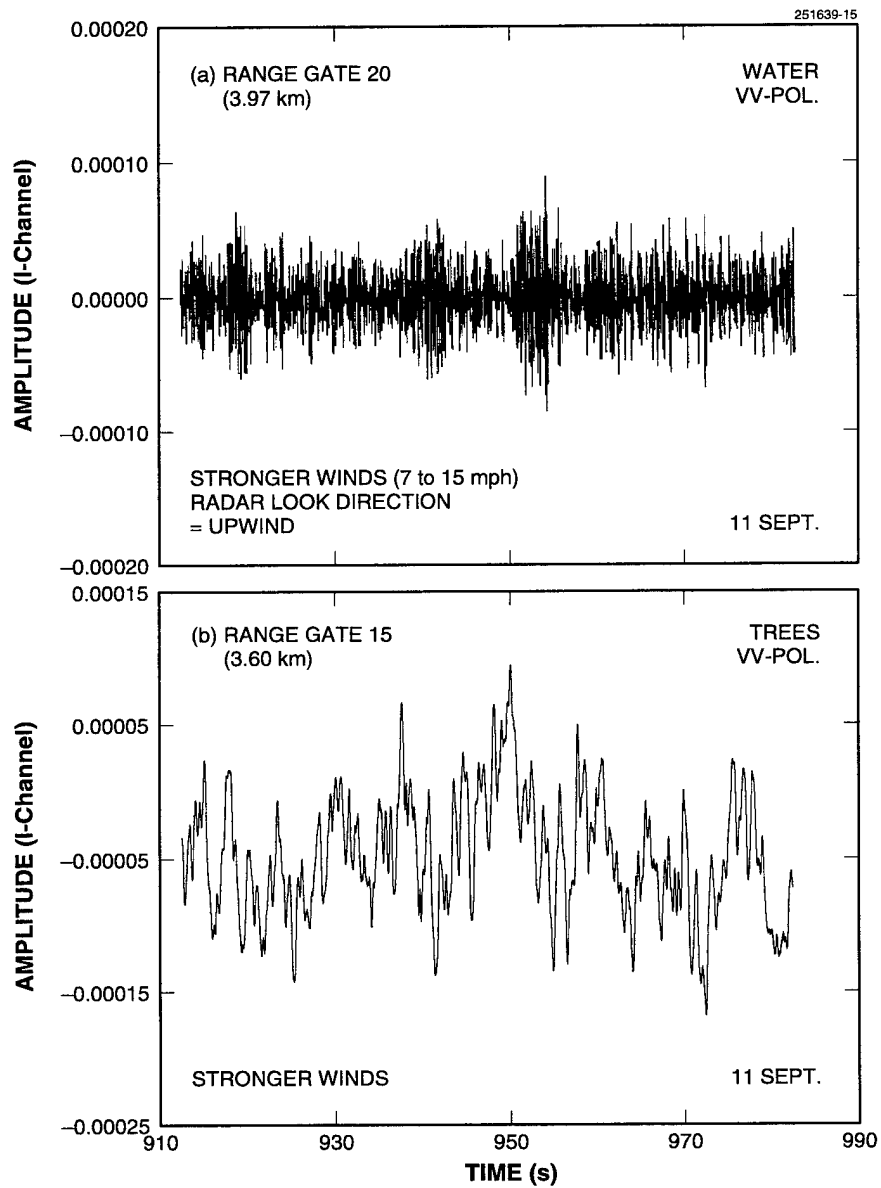


Figure 12. LCE-measured clutter amplitude temporal records, 11 September, VV-pol., (a) range gate 20 (3.97 km), water (Mare Meadow Reservoir) and (b) gate 15 (3.60 km), trees (near shore).

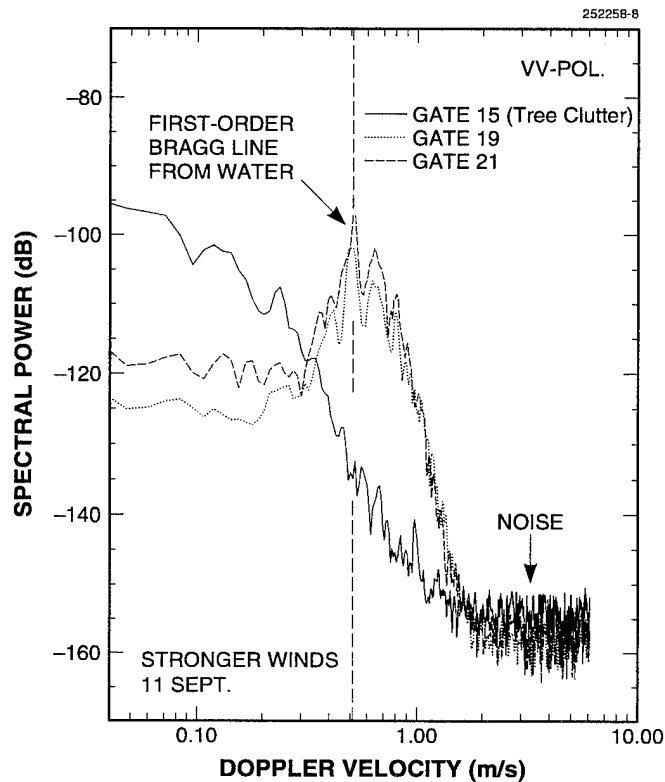


Figure 13. LCE-measured clutter power spectra showing variations with range as range gate position traverses Mare Meadow Reservoir, 11 September, VV-pol., gate 15 (3.60 km), trees.; gate 19 (3.90 km), water; gate 21 (4.05 km), water.

Variations in gate 20 water clutter spectra with polarization for the 11 September windier day are shown in Figure 14, in a manner paralleling the light-winds day results shown in Figure 8. The windier day HH-pol. water clutter in Figure 14 is stronger than in the corresponding light-winds day HH-pol. water clutter in Figure 8. Except for less dominant Bragg lines, the windier day results of Figure 14 are similar to the light-winds day results of Figure 8 with minor differences caused by differing wind conditions. The Bragg resonance phenomenon continued to be extensive in space across all seven water gates and persistent in time throughout the 22-min duration of measurements and across the complete polarization matrix of measurements on the windier day, as it was on the light-winds day.

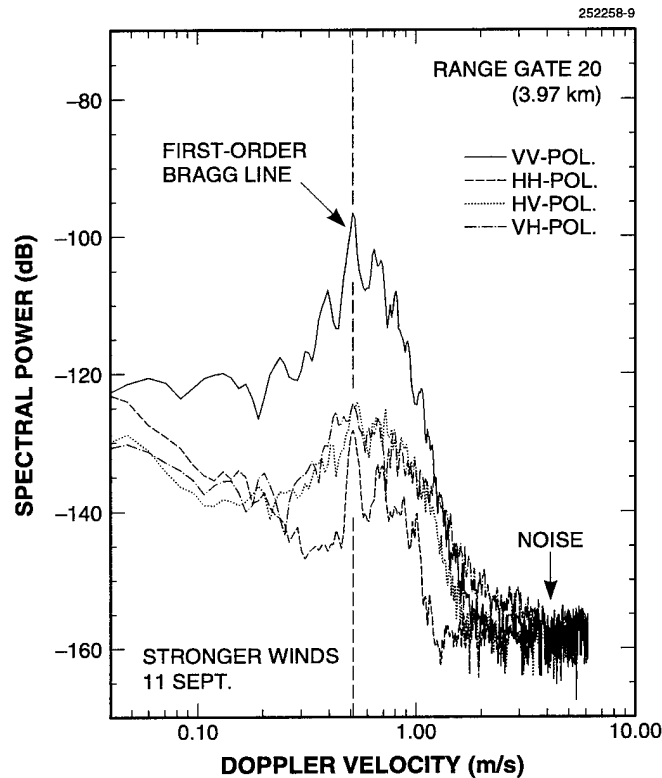


Figure 14. LCE-measured clutter power spectra from the surface of Mare Meadow Reservoir showing variations: VV-, HH-, HV-, and VH-pol., 11 September, range gate 20 (3.97 km).

Figure 15 illustrates the persistence in time of the Bragg resonance on 11 September by showing together results from the two VV-pol. experiments, in which the second commenced 13 min 14 s after the first. The earlier spectrum in Figure 15 is the 11 September spectrum shown in Figures 10 and 11. Although the Bragg resonance peak persists in both spectra in Figure 15, the details in spectral structure around the Bragg peak differ more in the two 11 September spectra of Figure 15 than in the two 5 September spectra of Figure 9. In particular, the later spectrum in Figure 15 has a spectral tail extending to higher Doppler velocities than the tail of the earlier spectrum. By chance, for $|v| > \approx 0.5$ m/s this extended tail of the later water clutter spectrum of Figure 15 is rather similar to the tail over the same Doppler interval of the widest LCE tree clutter spectra of Figure 3(b).

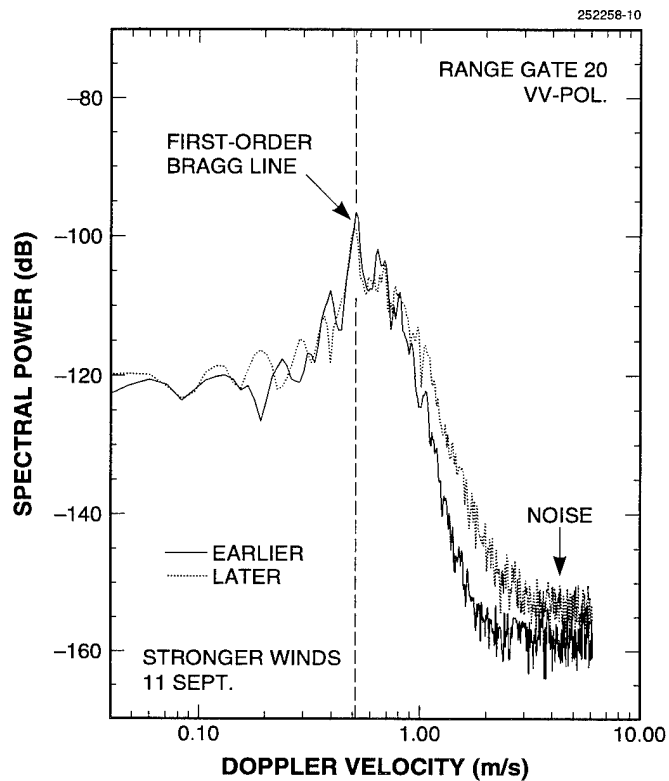


Figure 15. LCE-measured clutter power spectra from the surface of Mare Meadow Reservoir for two similar experiments showing variation with time of measurement, 11 September, VV-pol., range gate 20 (3.97 km). Later measurement performed 13 min 14 s after earlier measurement.

4. DISCUSSION

4.1 BRAGG SCATTERING IN SEA CLUTTER

In 1955 Crombie [19] measured sea clutter with an HF radar and correctly interpreted the dominant components he observed in the Doppler spectrum as Bragg resonances arising from water waves of one-half the radar wavelength. Since then, an extensive literature concerning this HF phenomenon has sprung up, motivated by the possibility of measuring surface currents and ocean waves at great distances with HF sky- or surface-wave radars. A recent succinct summary of the present state of development of this technology is provided in Tucker [2]. Figure 16 shows typical HF sea clutter spectra with strong Bragg resonances, which look very like the LCE spectra from Mare Meadow Reservoir shown in this report. The remote measurement of ocean surface currents by this HF radar technique, as a constant offset of the first-order Bragg spikes from their predicted, symmetrical positions (in the absence of currents) to either side of zero-Doppler [see Figure 16(b)] is now well established. The remote measurement of ocean wave conditions (i.e., directional wave spectra, wave amplitudes, sea state, etc.) depends on the higher-order Bragg resonances. The theoretical interpretation of the higher-order resonances, much of which has been developed by Barrick [3,16] is highly complex, and the practical consequences of obtaining useful information about ocean waves (as opposed to currents) by this technique have so far been limited. Three main radars have been used over the years to advance understanding of HF radar remote sensing of sea currents and waves [2], the most recent one being operated by the University of Birmingham, primarily for wave measurement [20,21].

Literature also exists concerning the use of microwave radar backscatter to obtain information about ocean surfaces. Recent articles on this subject include Plant and Keller [4] and Thompson [22]. A principal motivation of such studies is the potential use of satellite-borne synthetic aperture radars for providing information about ocean waves [5]. At microwave frequencies, ocean clutter spectra are generally broad and featureless, showing no peaks that could be interpreted as Bragg lines because long ocean waves (i.e., swells) have back-and-forth horizontal, as well as vertical, components resulting in orbital motions of water particles. These long-wave horizontal motions modulate the motion of the short ocean waves, which give rise to Bragg resonance at microwave frequencies. As a result, Bragg resonances in microwave ocean clutter spectra are often broadened and smeared out to the point where Bragg lines can no longer be resolved. However, a recent paper [4] shows that this is not always the case and indicates under what ocean conditions Bragg peaks and splittings can exist in microwave Doppler spectra of sea clutter.

Figure 17 reproduces some of Chan's [15] sea clutter measurements taken with the Lincoln Laboratory Phase One multifrequency radar at North Truro, Massachusetts, during a relatively calm sea (i.e., sea state = 2, wave height \cong 2 ft, wind speed \cong 5 kn). The Phase One sea clutter Doppler spectra at L-band and VHF, shown in Figures 17(a) and (b), respectively, do, indeed, show evidence of Bragg double peaks, although these peaks are not as sharp as the LCE Bragg spikes from Mare Meadow Reservoir. Figure 17(c) shows North Truro L-band measurements of sea clutter backscattering coefficient σ° as a function of grazing angle. In the data of Figure 17(c), σ° is stronger at VV- than HH-pol. by \approx 30 dB, a difference similar to that observed in the Mare Meadow Reservoir data. Although the σ° results of Figure 17(c) for 4° grazing angle are stronger than the LCE Mare Meadow Reservoir σ° results, other L-band, VV-pol., 4° grazing angle, sea state 2, σ° results exist [1,17,18], some of which [17,18] happen to be almost identical (viz., $\sigma^{\circ} = -47, -48$ dB) to the LCE reservoir results (viz., $\sigma^{\circ} = -48, -50$ dB). This finding may be fortuitous, considering the 2-ft swell on the ocean under sea state 2 that was lacking, of course, on the reservoir.

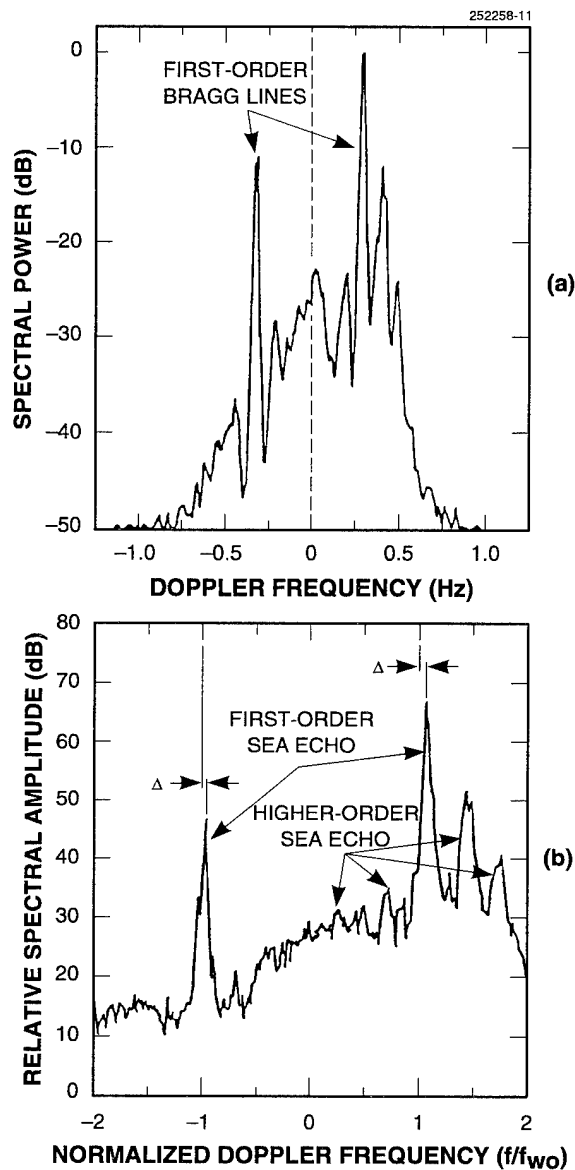


Figure 16. Published measurements of HF sea clutter spectra showing strong Bragg resonances. (a) Taken from Tucker [2]. Spectrum obtained with the University of Birmingham HF radar at 9 MHz. The energy for directional wave measurement is that in the relatively broad bands to either side of the first-order Bragg resonant peaks. (b) Taken from Barrick et al. [3] and shown also in Plant and Keller [4]. Spectrum obtained at 9.4 MHz. The first-order Bragg Doppler shift $f_{w0} = 0.31$ Hz; Δ is an offset due to surface current.

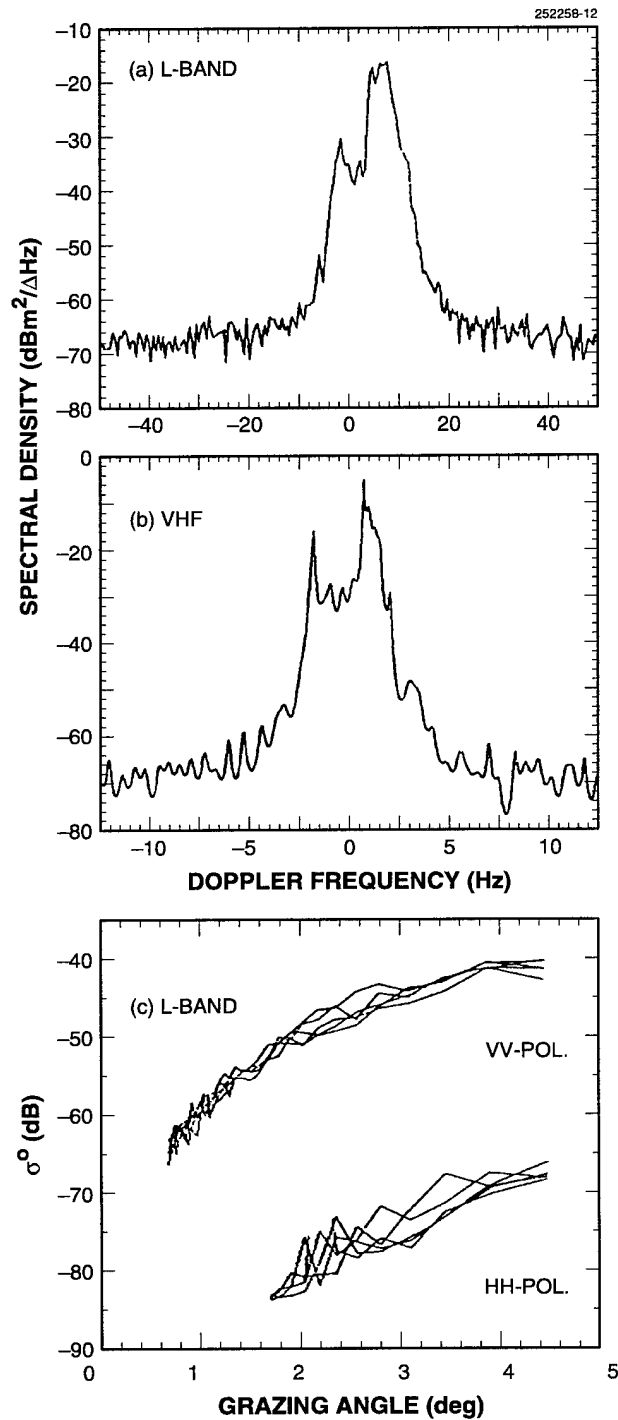


Figure 17. Phase One sea clutter measurements taken from Chan [15]. Measurements obtained under low, sea state 2 conditions (2-ft wave heights). (a) L-band spectrum with broad Bragg resonances, VV-pol., 1245 MHz; (b) VHF spectrum with narrower Bragg resonances, VV-pol., 168 MHz; (c) σ^0 versus grazing angle, L-band, VV- and HH-pol.

Over the years, Bragg scattering ideas about microwave backscatter from the sea have received their strongest support from wave-tank studies involving both paddle- and wind-generated waves but in which long-wave ocean swell does not occur. Sharp Bragg resonance lines have been routinely observed in microwave Doppler spectra obtained in wave tanks [4]. Such studies have been used in the development of composite surface scattering theory to explain microwave sea clutter [23]. The LCE measurements showing sharp Bragg resonances in the L-band backscatter from Mare Meadow Reservoir, as reported herein, would seem to fall within this latter subject area of Bragg scattering from wave tanks at microwave frequencies. For the measurements discussed in this report, Mare Meadow Reservoir (about 2 km long by about 0.6 km across) acts like a very large wave tank, allowing wind-generated gravity waves without the long-wave swell that exists on the open ocean and often masks Bragg resonances in microwave Doppler spectra.

4.2 CONTEXT FOR LAND CLUTTER

In recent years, there has been increased interest in specifying an overall environment clutter model that would include the Doppler interference from such things as aurora, meteor trails, cosmic noise, wind-blown material (e.g., leaves, dust, spray), birds, insects, rotating structures, rain, lightning, clear air turbulence, fluctuations of refractive index, etc. Such phenomena are often highly transient as they occur in measurements of radar Doppler spectra so that it is difficult to causally and quantitatively associate spectral artifacts directly with their sources.

In contrast, the nonzero-Doppler Bragg spikes measured from Mare Meadow Reservoir represent a concrete example of total environment clutter over land that is atypical of ground clutter in general and for which the cause can be definitively specified. The power levels at VV-pol. in the Mare Meadow Reservoir water clutter spectra are not inconsequential, as indicated by the three shown in Figure 18. Each spectrum was individually discussed previously in this report; spectrum (a) is from data taken on the light-winds day, and spectra (b) and (c) are from data taken 13 min apart on the stronger winds day. Thus the figure summarizes that significant spectral power at low but nonzero-Doppler velocities exists in inland water clutter spectra at VV-pol.

The water clutter spectra in Figure 18 may be compared with the tree clutter spectra in Figure 19. Figure 19 plots together the VV-pol. tree clutter spectra from gate 15 on the near shoreline of Mare Meadow Reservoir for both the light-winds day of 5 September and the stronger winds day of 11 September, as shown in Figures 7⁶ and 13, respectively. These two tree clutter spectra were measured simultaneously (i.e., same experiments) with the corresponding water clutter spectra of Figure 18(a) and (b). Also included for comparison in Figure 19 is one of the widest LCE tree clutter spectra ever measured, previously shown in Figure 3(b). This spectrum was also measured on 11 September but in a cell 10.8 km distant from the reservoir and 30 min later. At the LCE radar position on Wachusett Mt., 11 September was considered a strong, windy day in contrast to 5 September, which was considered only a breezy day. These qualitative assessments of wind conditions are borne out in the gate 15 tree clutter spectra shown in Figure 19 in that the 11 September spectra are wider than the 5 September spectrum.

⁶Figure 7 shows the left side of the spectrum; Figure 19 shows the right side.

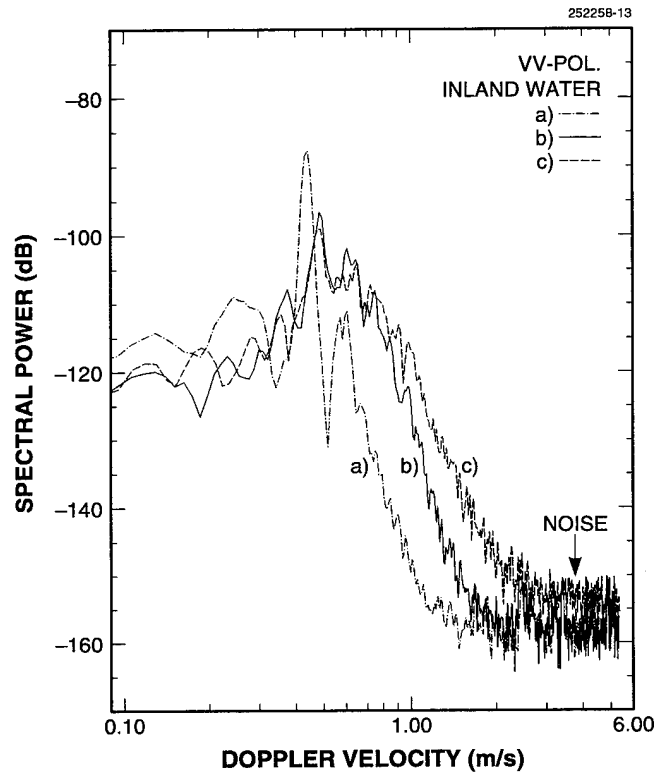


Figure 18. Three inland water clutter spectra at VV-pol.: (a) 5 and (b) 11 September; and (c) 11 September, 13 min 14 s later.

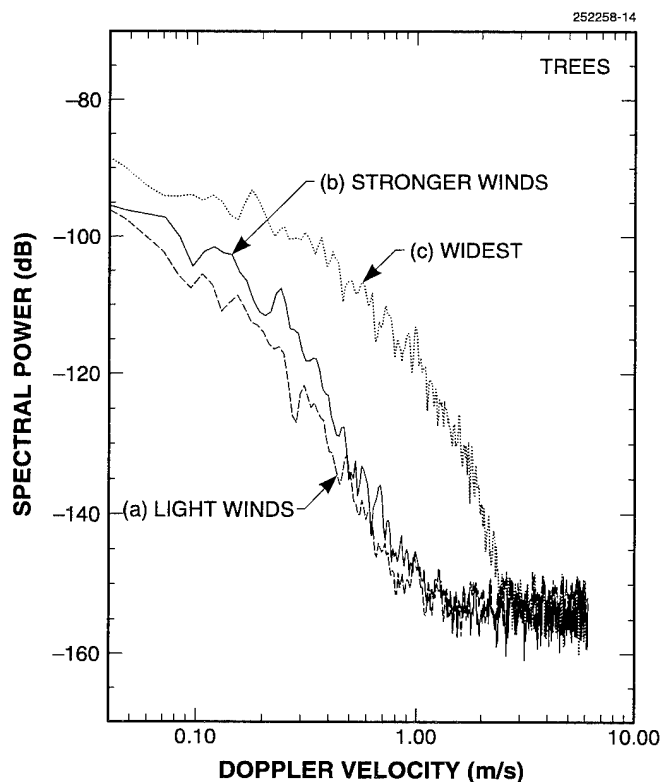


Figure 19. Three ground clutter spectra from trees at VV-pol.: (a) near shoreline of Mare Meadow Reservoir on 5 September (3.60 km), (b) near shoreline on 11 September (3.60 km), and (c) widest measured LCE spectrum, 11 September (7.94 km).

Figure 20 summarizes the differences between the water clutter power spectra in Figure 18 and the neighboring tree clutter power spectra in Figure 19. Figure 20 may be compared with Figures 7 and 13, which also show tree and water spectra together. In Figure 20, if the water clutter spectra (a), (c), and (e) are first compared with the tree clutter spectra (b) and (d) that were measured time-coincidentally in nearby cells, it is observed that water clutter spectral power far exceeds that of tree clutter by as much as 30 to 40 dB over a range of Doppler velocities from about 0.3 or 0.4 to 2 or 3 m/s, even though total tree clutter spectral power is 10 dB greater than total water clutter spectral power in these comparisons. Even if the widest tree clutter spectrum (f) ever measured by the LCE radar (from a 10.8-km distant cell 30 min later) is included, the water clutter spectral power still exceeds it by as much as 15 dB near the Bragg resonances over a range of Doppler velocities from about 0.4 or 0.5 m/s to as much as about 1/m/s in the case of measurement (e).

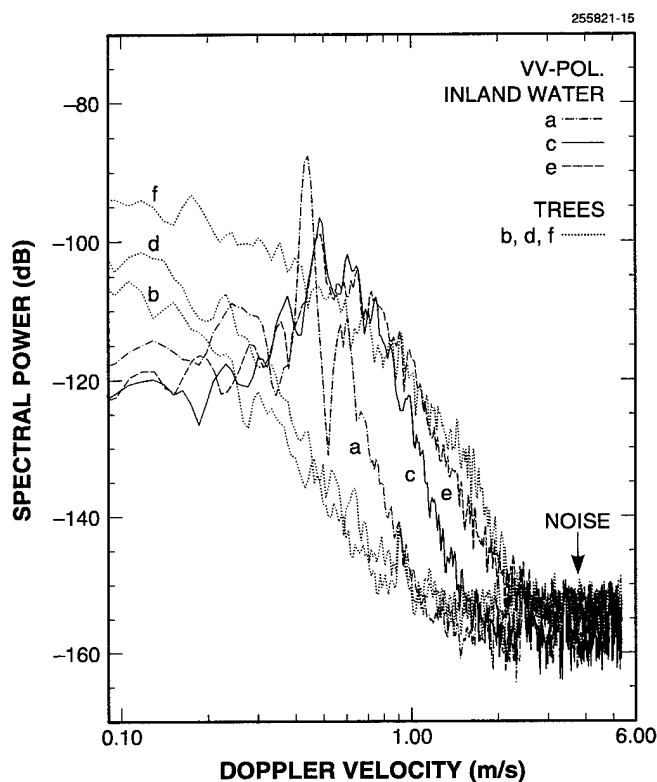


Figure 20. Inland water clutter versus tree clutter spectra: (a) water and (b) nearby trees on 5 September, (c) water and (d) nearby trees on 11 September, (e) water 13 min 14 s later, and (f) distant trees (widest) 29 min 52 s later.

In ground clutter modeling, it may be desired to compare the six spectra of Figure 20 on the basis of equivalent ac spectral power in each spectrum to separate the effects on spectral power level of differing σ^0 and ratio of dc/ac power from the intrinsic effects of differing spectral shape. Each spectrum in Figure 20 may be adjusted so that the total ac power in each measured spectrum is unity, and to show spectral power per infinitesimally small Doppler velocity interval $d\nu$ (i.e., dBW/d ν) for comparison with analytic spectral shapes, by means of the following additive term (i.e., vertical scale shift) in decibels for spectra (a) through (f), respectively: 104.2, 101.4, 106.3, 101.2, 107.8, and 95.6. The relative effects of these adjustments, for example, with respect to spectrum (a), is that spectra (c) and (e) are raised by 2.1 and 3.6 dB, respectively; and spectra (b), (d), and (f) are lowered by 2.8, 3, and 8.6 dB, respectively. Thus all these normalization adjustments, most of which are minor except for that of spectrum (f), increase relative water clutter spectral power with respect to relative tree clutter spectral power when shown on an equivalent total ac spectral power basis.

Conceptually, high enough tree clutter σ° combined with strong enough winds (strong winds lead to low ratios of dc/ac spectral power and wide normalized spectral shapes in treed cells) can result in clutter power spectral density from a treed cell exceeding clutter power spectral density from a neighboring water cell at the Bragg frequency. The spectral shapes of Figure 20 (when normalized by the preceding adjustment factors) indicate that tree clutter σ° must exceed water clutter σ° by ≈ 25 dB for the spectral density in the widest LCE tree spectrum (f) to equal the spectral density of the water spectrum (a) at the Bragg frequency, requiring tree clutter $\sigma^\circ \cong -25$ dB, since Mare Meadow Reservoir water clutter $\sigma^\circ \cong -50$ dB. Although tree clutter σ° is typically less than ≈ -25 dB at the generally low illumination angles of ground-based radar (e.g., for L-band at grazing incidence, mean tree clutter $\sigma^\circ = -32$ dB for both VV- and HH-pol. [24]), at higher angles tree clutter σ° can approach ≈ -25 dB (e.g., for L-band at depression angle = 4° , mean tree clutter $\sigma^\circ = -26$ dB for both VV- and HH-pol. [24]⁷). Thus under extremely windy situations [i.e., as typified by spectrum (f) in Figure 20], tree clutter spectral density may be expected to approach water clutter spectral density in a neighboring cell at the Bragg frequency. Under more normal situations [i.e., as typified by the much narrower tree clutter spectra (b) and (d) in Figure 20], water clutter spectral density in the vicinity of the Bragg line is expected to always exceed neighboring tree clutter spectral density in the Bragg frequency vicinity by large amounts.

Consider briefly how the results of Figure 20 might apply at other radar frequencies. Except for differing amounts of dc component, the relative shapes of ac clutter Doppler spectra from windblown trees when plotted against Doppler velocity (as opposed to Doppler frequency) x -axes are largely invariant with radar wavelength [6–8]. In contrast to the relative invariance of tree clutter velocity spectra with radar wavelength λ , the equivalent Doppler velocity at which Bragg resonance in water clutter spectra is expected to occur varies as $\sqrt{\lambda}$. Nevertheless, Bragg resonant Doppler velocities are expected to remain well within the range of tree clutter ac spectral power at other frequencies. For example, at VHF (e.g., 170 MHz) and X-band (e.g., 9100 MHz), the expected Bragg resonant Doppler velocities are 1.17 and 0.16 m/s, respectively. These Bragg resonant Doppler velocities are still within the range for which discernible ac tree clutter power was observed in VHF and X-band tree clutter spectra measured by Lincoln Laboratory's Phase One multifrequency clutter measurement radar [6,7]. The power levels that might be measured from inland water at frequencies other than L-band are conjectural at this time. Chan's [15] multifrequency sea clutter data obtained with the Phase One radar indicate that VV-pol. σ° increases from L-band at lower (i.e., UHF and VHF) and higher (i.e., X-band) frequencies and that the weak HH-pol. σ° at VHF, UHF, and L-band increase to approximate equivalence with VV-pol. σ° at X-band.

Small inland bodies of water are common in many geographical regions. There is no reason to believe that the measurement conditions under which Bragg resonance was observed from Mare Meadow Reservoir

⁷The most salient aspect of low-angle ground clutter is variability. Over the hilly forested terrain of the 294° radial at Wachusett Mt., the L-band, VV-pol., clutter coefficient σ° ranges from ≈ -15 to ≈ -40 dB. (Here, propagation effects are included in σ° .) The near shoreline of Mare Meadow Reservoir, which is close to being masked by intervening terrain between the radar and the reservoir, has $\sigma^\circ \cong -39$ dB. If the near shoreline were exactly on the theoretical shadow boundary of a single knife edge, there would be a 12-dB diffraction loss in clutter strength; raising the near shoreline σ° by 12 dB yields $\sigma^\circ = -27$ dB, which is close to the -26 dB value expected for L-band, low-relief forested terrain, 4° depression angle [24]. The steeply rising terrain along the far shoreline of the reservoir has $\sigma^\circ \cong -20$ dB. The cell that provided the widest LCE spectrum [i.e., Figure 20(f)] had $\sigma^\circ = -30$ dB.

were in any way unusual or "just right." Bragg resonance was seen in all seven cells occurring on this inland body of water throughout the 15- and 22-min measurement periods of two measurement days. However, since inland bodies of water occur at low elevations with respect to the surrounding terrain, they may often be masked to ground-based radar. Small inland bodies of water regularly become visible to airborne radars of overflying aircraft, although usually at relatively short range and at depression angles significantly above grazing incidence. Similarly, satellite-borne radars would also routinely observe small inland bodies of water but also at higher depression angles. Thus remote sensing radars with their higher depression angles might see small inland bodies of water more frequently than long-range surveillance radars, and the Bragg lines may be more noticeable at higher angles in tree clutter backgrounds since water clutter σ° rises faster with increasing grazing angle than does tree clutter σ° .

Within the recent increased interest in land clutter, specific attention motivated by advanced detection technology concerns has been devoted to the detailed characteristics of ground clutter spectra at very low but nonzero-Doppler frequencies and how these characteristics vary with time. These concerns can particularly involve, but are not limited to, bistatic measurement geometries. The first-order L-band Bragg resonant spikes observed from Mare Meadow Reservoir exist centrally within this Doppler interval of interest in L-band ground clutter spectra and are expected to stay within the ground clutter Doppler interval at other radar frequencies. Thus the occasional spatial occurrence of such spikes change what is otherwise expected for temporal statistical behavior of general land clutter spectra. In contrast to transient variations that can occur in clutter spectra from land clutter cells containing windblown foliage, the existence of Bragg spikes from land clutter cells known to be inland water may be largely invariant in space and time and outside the general range of variation of windblown foliage spectra. The extent to which Bragg spikes from small inland bodies of water might cause false alarms for moving target indicator or other Doppler signal processing techniques or algorithms designed for detecting and tracking targets in ground clutter requires further study.

5. SUMMARY

L-band radar backscatter measurements were recorded from the surface of a small inland fresh water reservoir in central Massachusetts on two measurement days under differing wind conditions. The measurements were conducted over a full polarization matrix (i.e., HH, VV, HV, VH). The measurement radar was sited on Wachusett Mt., 1000 ft above the surrounding hilly forested terrain. The reservoir was at 4-km range and 4° depression angle with respect to the radar. The clutter Doppler spectra of returns from water cells on the reservoir surface were considerably different from typical clutter Doppler spectra of returns from surrounding land cells containing windblown foliage. In particular, the water spectra contained strong Bragg resonant components at low (i.e., 3 to 4 Hz) but nonzero-Doppler frequencies. In addition to the dominant first-order Bragg component existing at negative Doppler when the water waves were receding from the radar (first measurement day) or at positive Doppler when the water waves were approaching the radar (second measurement day), a split component also existed on both measurement days at approximately the image frequency of the dominant component (i.e., on both days, components existed at $\approx \pm f_b$, where f_b is the Bragg resonant frequency). The two image components did not exist at exactly mirror image frequencies $\pm f_b$ because of surface currents. The exact Doppler frequencies at which the principle and split first-order Bragg components occurred were, on the first measurement day, -3.8 and +3.4 Hz; and on the second measurement day, +4.2 and -3.0 Hz, respectively.

On the first measurement day, winds were light. Strong, highly developed Bragg resonance existed in the VV-polarized backscatter data obtained that day. Sharp narrow first-order Bragg spikes rose 20 to 25 dB above adjacent spectral levels in the Doppler spectra of this VV-polarized backscatter. The maximum amplitude of the dominant Bragg spike at -3.8 Hz was 40 to 45 dB stronger than tree clutter at -3.8 Hz in nearby spatial cells containing windblown trees and only 10 dB weaker than the peak zero-Doppler tree clutter in the same nearby cells.

On the second measurement day, winds were stronger. Significant Bragg resonance continued to exist in the VV-polarized backscatter data obtained that day, but the absolute levels of the Bragg spikes were 10 dB weaker than on the light-winds day. Still, the dominant Bragg spike at +4.2 Hz on the second day was 35 dB stronger than tree clutter at +4.2 Hz in nearby cells and only 12 dB weaker than the peak zero-Doppler tree clutter in those cells. The zero-Doppler tree clutter return was also reduced under the windier conditions.

On both measurement days significant Bragg resonance occurred in the returns at all four combinations of polarization—HH, VV, HV, and VH. However, the backscatter at HH-polarization was 30 dB or more weaker than at VV-polarization, as expected for L-band returns from water surfaces. The cross-polarized returns (i.e., at HV and VH polarization) were at intermediate levels between the strong VV- and weak HH-polarization levels. Bragg resonance persisted throughout the course of measurements on both measurement days (15 min on the first day, 22 on the second) and for all seven range gates from near- to far-side across the reservoir surface.

Current interest exists in the various types of clutter that can occur over land, including Doppler interference from occasional spectral artifacts. This report illustrates that inland water cells have quite different L-band clutter Doppler spectra than more commonly occurring windblown foliage cells. Advanced

detection technology concerns can focus interest on the expected characteristics of ground clutter at low Doppler frequencies. Within this Doppler regime, strong Bragg spikes at VV-polarization from occasional inland water cells do not fall within the generally expected statistical variability of windblown foliage cells under typically occurring wind conditions. The possibility exists that nonzero-Doppler Bragg spikes in inland water clutter spectra might cause false alarms for detection algorithms focusing on the low Doppler regime of ground clutter.

REFERENCES

1. M.W. Long, *Radar Reflectivity of Land and Sea*, 2nd ed., Boston, Mass.: Artech House, Inc. (1983).
2. M.J. Tucker, *Waves in Ocean Engineering*, Chichester, England: Ellis Horwood, Ltd. (1991).
3. D.E. Barrick, J.M. Headrick, R.W. Bogle, and D.D. Crombie, "Sea backscatter at HF: interpretation and utilization of the echo," *Proc. IEEE* **62**, 673-680 (1974).
4. W.J. Plant and W.C. Keller, "Evidence of Bragg scattering in microwave Doppler spectra of sea return," *J. Geophys. Res.* **95**, 16299-16310 (1990).
5. J.W. Wright, "Detection of ocean waves by microwave radar; the modulation of short gravity-capillary waves," *Boundary Layer Meteorol.* **13**, 87-105 (1978).
6. J.B. Billingsley and J.F. Larrabee, "Measurements of Radar Ground Clutter Power Spectra in Forest and Desert Terrains," Lexington, Mass.: MIT Lincoln Laboratory, Technical Rep. 997 (in preparation).
7. J.B. Billingsley, "A model for spectral spreading due to intrinsic motion in windblown radar ground clutter," for submission to *IEEE Trans. AES* (in preparation).
8. J.B. Billingsley and J.F. Larrabee, "Measured Spectral Extent of L- and X-Band Radar Reflections from Windblown Trees," Lexington, Mass.: MIT Lincoln Laboratory, Project Rep. CMT-57 (6 February 1987), DTIC AD-A179942/8.
9. J.B. Billingsley and J.F. Larrabee, "Multifrequency Measurements of Radar Ground Clutter at 42 Sites," Lexington, Mass.: MIT Lincoln Laboratory, Technical Rep. 916, Vols. 1, 2, 3 (15 November 1991).
10. R.L. Ferranti, "Very low phase noise in a pulsed 10-kw L-band triode power amplifier," Santa Clara, Calif.: *Proc. RF Expo West*, 59-66 (February 1991).
11. F.J. Harris, "On the use of windows for harmonic analysis with the discrete Fourier transform," *Proc. IEEE* **66**, 51-83 (January 1978).
12. E.J. Barlow, "Doppler radar," *Proc. IRE* **37**, 4 (1949).
13. W. Fishbein, S.W. Graveline, and O.E. Rittenbach, "Clutter Attenuation Analysis," Fort Monmouth, N.J.: U.S. Army Electronics Command, Technical Rep. ECOM-2808 (March 1967). Reprinted in *MTI Radar*, D.C. Schleher, Boston, Mass.: Artech House, Inc. (1978).
14. W.L. Simkins, V.C. Vannicola, and J.P. Ryan, "Seek Igloo Radar Clutter Study," Rome Air Development Center, Technical Rep. RADC-TR-77-338 (October 1977). Updated in FAA-E-2763b Specification, Appendix A (May 1988). See also FAA-E-2763a (September 1987), FAA-E-2763 (January 1986, July 1985).

15. H.C. Chan, "Radar sea clutter at low grazing angles," *IEEE Proc.* **137**, 102–112 (1990).
16. D.E. Barrick, "Remote sensing of sea state by radar," in V. E. Derr, ed., *Remote Sensing of the Troposphere*, Washington, D.C., U.S. Govt. Printing Office (1972).
17. M.M. Horst, F.B. Dyer, and M.T. Tuley, "Radar sea clutter model," *Int. Conf. Ant. Propag.*, London: IEEE Conf. Pub. No. 169, 6–10 (1978).
18. F.E. Nathanson, "*Radar Design Principles*," 2nd ed., New York: McGraw-Hill (1991).
19. D.D. Crombie, "Doppler spectrum of sea echo at 13.56 Mc/s," *Nature* **175**, 681–682 (1955).
20. E.D. Shearman and L.R. Wyatt, "High frequency ground-wave radar remote measurement of ocean wave and current parameters in the Celtic Sea: Project NURWEC 2," *Proc. Fifth Int. Conf. Electronics for Ocean Technol.*, IERE Conf. Pub. No. 72, 165–173 (1987).
21. L.R. Wyatt, "High frequency radar measurements of the ocean wave directional spectrum," *IEEE J. Ocean. Eng.* **16**, 163–169 (1991).
22. D.R. Thompson, "Calculation of microwave Doppler spectra from the ocean surface with a time-dependent composite model," in G.J. Komen and W.A. Oost, eds., *Radar Scattering from Modulated Wind Waves*, Netherlands: Kluwer Academic (1989).
23. J.W. Wright, "A new model for sea clutter," *IEEE Trans. Ant. Propag.* **AP-16**, 217–223 (1968).
24. J.B. Billingsley, "A Handbook of Multifrequency Land Clutter Coefficients for Surface Radar," Lexington, Mass.: MIT Lincoln Laboratory, Technical Rep. 958 (in preparation).

REPORT DOCUMENTATION PAGE

Form Approved
OMB No. 0704-0188

Public reporting burden for this collection of information is estimated to average 1 hour per response, including the time for reviewing instructions, searching existing data sources, gathering and maintaining the data needed, and completing and reviewing the collection of information. Send comments regarding this burden estimate or any other aspect of this collection of information, including suggestions for reducing this burden, to Washington Headquarters Services, Directorate for Information Operations and Reports, 1215 Jefferson Davis Highway, Suite 1204, Arlington, VA 22202-4302, and to the Office of Management and Budget, Paperwork Reduction Project (0704-0188), Washington, DC 20503.

1. AGENCY USE ONLY (Leave blank)	2. REPORT DATE 1 August 1995	3. REPORT TYPE AND DATES COVERED Technical Report	
4. TITLE AND SUBTITLE Bragg Resonance in Measured L-Band Radar Clutter Doppler Spectra from Inland Water		5. FUNDING NUMBERS C — F19628-95-C-0002 PR — 331 PE — 63003F	
6. AUTHOR(S) J. Barrie Billingsley and John F. Larrabee		7. PERFORMING ORGANIZATION NAME(S) AND ADDRESS(ES) Lincoln Laboratory, MIT 244 Wood Street Lexington, MA 02173-9108	
8. PERFORMING ORGANIZATION REPORT NUMBER TR-1019		9. SPONSORING/MONITORING AGENCY NAME(S) AND ADDRESS(ES) Department of the Air Force ARPA SAF/AQL 3701 N. Fairfax Dr. The Pentagon Arlington, VA 22203-1714 Washington, DC 20330	
10. SPONSORING/MONITORING AGENCY REPORT NUMBER ESC-TR-95-018		11. SUPPLEMENTARY NOTES None	
12a. DISTRIBUTION/AVAILABILITY STATEMENT Approved for public release; distribution is unlimited.		12b. DISTRIBUTION CODE	
13. ABSTRACT (Maximum 200 words) A highly developed Bragg resonance phenomenon was observed in measurements of vertically polarized L-band radar backscatter recorded from the surface of a small inland fresh-water reservoir in central Massachusetts. These measurements were obtained with Lincoln Laboratory's LCE (L-band Clutter Experiment) radar sited on Wachusett Mt. from which the reservoir surface was visible at 4-km range and 4° depression angle, on a day of light winds with the radar looking obliquely downwind. The highly developed Bragg resonance in the backscatter from the reservoir surface caused strong Bragg spikes to exist in the clutter Doppler spectrum from the reservoir at low (viz., +3.4 and -3.8 Hz) but nonzero-Doppler frequencies. The sharp narrow first-order Bragg spikes rose 20 to 25 dB above adjacent spectral levels in the clutter spectra from the reservoir surface. The maximum amplitude of the dominant Bragg spike at -3.8 Hz was 40 to 45 dB stronger than tree clutter at -3.8 Hz in nearby spatial cells and only 10 dB weaker than the peak zero-Doppler tree clutter in the same nearby cells. This strong Bragg resonance at vertical polarization was persistent in time (15 min) and space (all seven range gates for which the reservoir surface was visible to the radar) throughout the course of measurements on the light-winds measurement day. Spectral results are presented for both cross-polarized and both copolarized combinations of linear polarization. Bragg spikes were observed to exist across this polarization matrix of measurements, although at horizontal polarization the overall backscatter from the reservoir surface, including the Bragg resonant component, was much weaker than at vertical polarization. On a second measurement day of stronger winds and changed wind direction (such that the radar was looking upwind), significant Bragg resonance still existed in the backscatter from the reservoir surface but was weaker than on the light-winds day. Strong Bragg spikes at low but nonzero-Doppler frequencies from small inland bodies of water might potentially cause false alarms for moving target indicator or other Doppler signal processing techniques designed for target detection in ground clutter.			
14. SUBJECT TERMS radar clutter lake backscatter clutter measurements inland water Bragg resonance Doppler frequency spectra power spectra terrain tree clutter microwave L-band			15. NUMBER OF PAGES 50
17. SECURITY CLASSIFICATION OF REPORT Unclassified			16. PRICE CODE
18. SECURITY CLASSIFICATION OF THIS PAGE Unclassified	19. SECURITY CLASSIFICATION OF ABSTRACT Unclassified	20. LIMITATION OF ABSTRACT Same as Report	